Hydrogen-based integrated energy and mobility system for a real-life office environment

Safaei Farahani, Samira; Bleeker, Cliff; van Wijk, Ad; Lukszo, Zofia

DOI
10.1016/j.apenergy.2020.114695

Publication date
2020

Document Version
Final published version

Published in
Applied Energy

Applied Energy 264 (2020) 114695

Contents lists available at ScienceDirect

Applied Energy

journal homepage: www.elsevier.com/locate/apenergy

Hydrogen-based integrated energy and mobility system for a real-life office environment☆

Samira S. Farahani[a,*], Cliff Bleeker[b], Ad van Wijk[b], Zofia Lukszo[a]

[a] Department of Engineering, Systems and Services, Delft University of Technology, 2628 BX Delft, the Netherlands
[b] Department of Process and Energy, Delft University of Technology, 2628 CB Delft, the Netherlands

HIGHLIGHTS

- Lowest system costs of energy with both hydrogen and electricity as energy carriers.
- System with only a hydrogen grid is cheaper than one with only an electricity grid.
- Between 20% to 30% of the consumed energy comes from the storage.
- Fuel cell vehicles are more flexible and cheaper for backup power than battery ones.
- Electric vehicles are feasible for balancing and backup power in an office building.

ARTICLE INFO

Keywords:
Integrated energy and mobility system
Hydrogen-based energy system
Vehicle-to-grid
Optimal scheduling
Techno-economic analysis

ABSTRACT

The current focus on the massive CO2 reduction highlights the need for the rapid development of technology for the production, storage, transportation and distribution of renewable energy. In addition to electricity, we need other forms of energy carriers that are more suitable for energy storage and transportation. Hydrogen is one of the main candidates for this purpose, since it can be produced from solar or wind energy and then stored; once needed, it can be converted back to electricity using fuel cells. Another important aspect of future energy systems is sector coupling, where different sectors, e.g. mobility and energy, work together to provide better services. In such an integrated system, electric vehicles – both battery and hydrogen-based fuel cell – can provide, when parked, electricity services, such as backup power and balancing; when driving they produce no emissions. In this paper we present the concept design and energy management of such an integrated energy and mobility system in a real-life environment at the Shell Technology Centre in Amsterdam. Our results show that storage using hydrogen and salt caverns is much cheaper than using large battery storage systems. We also show that the integration of electric vehicles into the electricity network is technically and economically feasible and that they can provide a flexible energy buffer. Ultimately, the results of this study show that using both electricity and hydrogen as energy carriers can create a more flexible, reliable and cheaper energy system at an office building.

1. Introduction

In recent years, the European Union has set ambitious targets towards a carbon-free energy transition. After the Paris Agreement of 2015 set a long-term goal of keeping the increase in global average temperature below 2°C above preindustrial levels and aimed to limit the increase to 1.5°C [1], many countries are now developing strict policies to reduce CO_2 and other greenhouse gas emissions significantly by 2050. Consequently, there is increasing interest worldwide in renewable energy production – mainly from solar and wind. The main challenges arising in this context are related to the intermittent nature of these sources, as well as the mismatch between supply and demand. For example, high wintertime heat demand in cold places, just when solar production is low. Hence, there is a great need to find alternative energy carriers alongside electricity. Hydrogen is one of the main candidates for this purpose since it can be produced from – generally cheap – solar and wind energy, it can be stored cheaply in salt caverns, it can be transported via ships and existing gas pipelines to the

☆ This research is supported by the NWO-URSES+ project Car as Power Plant-LIFE, which is financed by the Netherlands Organization for Scientific Research (NWO).

* Corresponding author.
E-mail address: samifarahani@gmail.com (S.S. Farahani).

https://doi.org/10.1016/j.apenergy.2020.114695
Received 2 November 2019; Received in revised form 13 February 2020; Accepted 16 February 2020
Available online 02 March 2020

consumption location and, finally, it can be converted back into electricity using fuel cells.

To achieve the goals set in the Paris Agreement, different sectors – energy, mobility, industry and so on – need to work together to speed up the required technological, societal and institutional changes. As such, sector coupling is an important aspect in the upcoming energy transition. This is when different sectors help each other to improve their services and capabilities. In this paper, our focus is sector coupling between energy and transport systems.

To integrate electricity and transport systems, we have developed a novel concept known as *Car as Power Plant* (CaPP) [2] to utilise automotive fuel cells as stationary power production units during non-driving hours (typically at home, or in parking lots during office hours). This involves using the car in what we refer to as the vehicle-to-grid (V2G) mode [3,4]. When parked, its fuel cell unit can deliver power back to the electricity grid to balance it, to offset peak demand or to serve as a baseload power generator. Hydrogen is used as a storage medium so as to decouple the supply of and demand for renewable power in terms of time and distance. CaPP has the potential to replace power plants worldwide, creating an integrated, efficient, reliable, flexible, clean and smart energy and transport system [5].

Recent studies have shown that the integration of energy and transport systems may create synergies in energy transition. As concluded in [6], the high benefit of grid expansion becomes weaker with tighter sector coupling. In [7], a commercial fuel cell electric vehicle and a battery electric vehicle are connected to a zero-energy building and their performance is compared. In [8], the integration of transportation energy with a net zero-energy community utilising captured waste hydrogen from chlor-alkali plants is examined. Integrating smart electricity, smart thermal and smart gas grids to enable 100% renewable energy and transport solutions has been studied in [9]. Moreover, an analysis of hydrogen-distributed energy systems with photovoltaics for load levelling and vehicle refuelling has been reported by the National Renewable Energy Laboratory of the US Department of Energy [10]. The role of hydrogen in low-carbon future energy systems has been studied by several researchers. For example, its crucial and complementary role in the future sustainable energy economy has been discussed in [11]. Hydrogen as an alternative energy carrier in a decarbonized energy system has been studied by both [12,13]. They conclude that hydrogen is an efficient energy vector for the transport and storage of renewable energy and is an enabler of sectoral integration within a decarbonization pathway. Moreover, [14,15] discuss the efficient storage of hydrogen in existing salt caverns. Finally, multi-carrier energy systems have already been designed, with a focus on electricity and natural gas or heat as their energy carriers [16,17].

In most of these studies, however, only battery-powered electric vehicles are considered as a means of energy storage and to deliver electricity back to the grid. Moreover, energy system designs discussed currently in the literature are mostly not integrated with the transport system as we are proposing here, with a significant role for fuel cell and battery electric vehicles in powering the building. Also, whilst some researchers have looked at multi-carrier energy systems, few so far have investigated the combination of electricity and hydrogen as the main carriers.

Our line of research focuses on the system level, and lately we have conducted several studies of the CaPP concept that include analyses of its operation and control, policies and regulations and economic feasibility. We have shown that reaching a fully renewable integrated energy and mobility system is both achievable and viable [18,19]. We have also studied the operational and control aspects of such a system [20,21], as well as institutional aspects of CaPP taking into account the behaviour of various actors in the energy system [22,23]. We have further shown that investing in such energy systems can be profitable for all parties involved [24].

To bridge the abovementioned gaps in the existing research, and as a further step building on our previous publications, this paper focuses on the concept design of the CaPP system in a real-life environment at the Shell Technology Centre in Amsterdam (STCA), which is a combined office and chemical laboratory building. Our work is diverse in its *novelty*: (1) it presents a tailored design for a real-life environment as a step towards wider implementation of such integrated systems in public places; (2) it uses both hydrogen and electricity as energy carriers and both fuel cell and battery electric vehicles for V2G purposes; (3) it provides a cost analysis of a coupled energy system taking into account the entire supply chain, including production, storage, transport and end users; and (4) it provides an optimal scheduling for the energy management of such a system, with the aim of minimising both production costs and – as an incentive to vehicle owners – degradation of fuel cells and batteries.

The energy system designed for the STCA is based on 100% renewable energy sources (solar and wind) and two energy carriers (electricity and hydrogen), together with electric vehicles (battery and hydrogen-based fuel cell) to deliver electricity back to the building's grid during parking hours for balancing and backup purposes. One important issue when dealing with renewable energy is its storage and the higher dependency of supply on that factor. In the current fossil-based energy system, 20% of all natural gas consumed each winter comes from underground storage [25]. One of our goals in this study is to show the extent to which the supply is dependent on storage in such an integrated energy and mobility system. In addition, we provide techno-economic analysis to evaluate the costs of such a system and provide an optimal scheduling for its energy management and improvement of its operational performance.

The paper is organised as follows. Section 2 describes the research methods used to design the energy system and to calculate its cost. Section 3 describes the energy system at STCA. In Section 4 we describe three possible scenarios and provide the results of our techno-economic and sensitivity analyses for each of them. Section 5 presents the optimal scheduling to minimise energy production costs as well as degradation of the production units. Finally, Section 6 presents our conclusions.

2. Research method

2.1. Approach

The research was conducted in a series of steps, as follows.

1. Design and dimensioning of the integrated energy and mobility system at the STCA, based on the requirements given in Section 2.2.
2. Analysing the annual energy demand of the office in two time frames: Near Future (2025–2030) and Mid-Century (2040–2050); see Section 3.
3. Defining different scenarios for each time frame, using different energy carriers (electricity and hydrogen) and different production and consumption units; see Section 4.
4. Calculating the annual energy balance for each scenario by matching demand with solar and wind power production, energy storage and different local production units; see Sections 2.3 and 4.
5. Determining the cost of energy for each scenario and for the two time frames by calculating: a) the total system cost of energy; b) the system levelized cost of energy; and c) the specific cost of energy for the STCA; see Sections 2.4 and 4.
6. Analysing the sensitivity of the cost of energy in the Mid-Century time frame in respect of the set of key assumptions and parameters used; see Sections 4.
7. Optimal scheduling for a systematic use of different production units in the system, with the aim of minimising the degradation costs of the batteries and fuel cells as well as the cost of energy production at the STCA; see Section 5.

2.2. Design requirements and dimensioning

The design of the energy system for the STCA fulfils the following design requirements: (1) its energy and transport systems use only

electricity and hydrogen as energy carriers; (2) the building uses both electricity and hydrogen for seasonal energy storage; (3) the system can be implemented in existing infrastructure and buildings; (4) it is dependent on a local underground hydrogen pipeline distribution network in the urban area; (5) it uses only renewable energy sources (local solar and large-scale wind); and (6) it is independent of natural gas and district heating grids or any expansion of these systems.

Section 3 describes the design and dimensioning of the energy system at the STCA. The dimensioning includes a wide range of relevant aspects such as the number of employees, the building's floor, roof and parking areas and the number of available vehicles.

2.3. Energy balance

Our analysis uses the STCA's energy consumption data, covering electricity per 15-min period and natural gas per hour. This data is collected from different consumption units in the building, such as heat pumps, the incinerator and lighting units, and we simulate the supply-demand profile of the energy system based upon it. The key goal of the design is to maintain the energy balance between supply and demand at every 15-min time step.

The first local energy production source at the office is solar. The maximum amount of solar power that can be generated is calculated from the STCA's available roof area, using the building plans. Due to insufficient solar generation capability and a mismatch with the building's load profile (mainly due to lab activities), additional wind power and energy storage are required. Moreover, we include local production options such as a stationary fuel cell and electric vehicles (EVs), both battery (BEVs) and fuel cell (FCEVs), delivering electricity to the building during their parked hours. Henceforth, whenever we refer to EVs delivering electricity to the grid we mean the building's local electricity grid.

A technology choice is made and then, for each scenario, an assessment is conducted covering the efficiencies, sizes, cost and required development time for all the components in the energy system. Component sizes are determined based on average load patterns and the energy balance is calculated taking into account the efficiencies of the different conversion and storage technologies concerned.

2.4. Cost of energy

To calculate the cost of energy at the office, we consider three components [1]:

- Total System Cost of Energy, TSCoE [€/year].
- System Levelized Cost of Energy for electricity $SLCoE_e$ [€/kWh], hydrogen $SLCoE_{H2}$ [€/kg], and heat $SLCoE_h$ [€/kWh].
- Specific Cost of Energy for Building $SCoE_B$ [€/m^2/year].

2.4.1. Total system cost of energy

The TSCoE in €/year is the sum of the Total annual capital and operation and maintenance Costs TC_i (€/year) of the n components at the energy system:

$$TSCoE\,(€/\text{year}) = \sum_{i=1}^{n} TC_i. \tag{1}$$

The TC_i of an individual component is calculated with the annual Capital Cost CC_i (€/year) and the Operation and Maintenance Cost OMC_i (€/year):

$$TC_i(€/year) = CC_i + OMC_i, \quad \text{for } i = 1, \ldots, n. \tag{2}$$

The CC_i (€/year) of a component is calculated with the annuity factor AF_i (%), installed component capacity Q_i (component specific capacity), and investment cost IC_i (€per component specific capacity):

$$CC_i(€/year) = AF_i \times Q_i \times IC_i, \tag{3}$$

where the annuity factor AF_i is based on the weighted average cost of capital WACC (%) and the economic lifetime of the component LT_i (years):

$$AF_i = \frac{WACC \times (1 + WACC)^{LT_i}}{[(1 + WACC)^{LT_i}] - 1}. \tag{4}$$

In this paper, the WACC of 3% is assumed[2] [26].

The annual OMC_i (€/year) is defined as an annual percentage OM_i (%) of Q_i and IC_i:

$$OMC_i(€/year) = OM_i \times Q_i \times IC_i. \tag{5}$$

2.4.2. System levelized cost of energy

The system levelized cost of energy for electricity $SLCoE_e$ (€/kWh), hydrogen $SLCoE_{H2}$ (€/kg), and heat $SLCoE_h$ (€/kWh) are calculated by allocating a share of the $TSCoE_{STCA}$ related to electricity $TSCoE_{STCA,\,e}$, hydrogen $TSCoE_{STCA,\,H2}$, or heat $TSCoE_{STCA,\,h}$. These shares are then divided by the annual electricity EC_e(kWh/year), hydrogen EC_{H2} (kg/year), or heat EC_h (kWh/year) consumption, respectively, and yields

$$SLCoE_e(€/kWh) = \frac{TSCoE_{STCA,e}}{EC_e} \tag{6}$$

$$SLCoE_{H2}(€/kg) = \frac{TSCoE_{STCA,H2}}{EC_{H2}} \tag{7}$$

$$SLCoE_h(€/kWh) = \frac{TSCoE_{STCA,h}}{EC_h}. \tag{8}$$

Note that the difference between levelized cost of energy and system levelized cost of energy is that in the latter, we include all transportation, storage, infrastructure, and distribution costs.

2.4.3. Specific cost of energy

The specific cost of energy is defined as the cost of energy per physical unit [27]. For the building's energy consumption, the $SCoE_B$ (€/m^2/year) is defined as the cost of the annual specific energy consumption (SEC_B) (kWh/m^2/year) by all the energy-consuming equipment within that building per square meter:

$$SCoE_B = SLCoE_e \times SEC_B. \tag{9}$$

3. System description and design

The real-life environment chosen for the concept design of the CaPP system is the Shell building in Amsterdam known as Shell Technology Centre (STCA), which is a combination of office space and a chemical laboratory. Located in the north of the city, it has a floor area of 76,136 m^2 and is the workplace for about 1000 employees. Its current energy system consists of three heat pumps with a total capacity of 3300 kW_{heat}, rooftop solar panels with a capacity of 51 kW_p and 1300 kVA diesel generators for emergency and backup power. It has an incinerator for lab waste and two parking lots with a total of 454 spaces, for both staff and visitors. The building is linked to the national electricity grid with a 10 MW-capacity connection.

The building's current demand profile for four representative months of the year (one in each season) is shown in the upper plot in Fig. 1. The lower plot shows the frequency of certain load demands over the course of one year. Due to its lab activities, this building has a higher load profile than the average office block in the Netherlands

[1] The rest of definitions are based on [19].

[2] The 3% WACC is based on 80% loan with 1.5% interest rate, and 20% own investment with 9% internal rate of return (IRR). This WACC falls within the low risk category of real state [26].

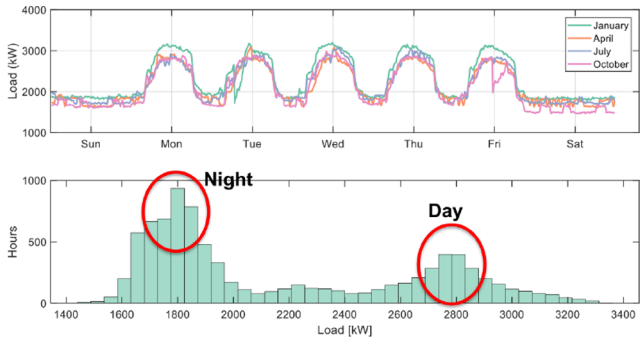

Fig. 1. Hourly demand profile and load distribution of the Shell office for a sample year.

Table 1
Share of energy between the office space and the chemical laboratory at the Shell office.

	Electricity	Natural Gas
Office (w/ heat pumps)	26%	58%
Laboratory	74%	42%
Total	19010 [MWh]	361329 [m^3]

[28]. The distribution of energy demand between the office space and the laboratory is presented in Table 1. From the load-profile data, we have calculated that 74% of the load is related to lab activities, 16% to office consumption (estimating 50,000 m^2 allocated as office space, with an annual demand of 60 kWh/m^2) and 10% to the heat pumps. Looking at natural gas consumption in the building, 42% is attributable to lab activities (mainly in the incinerator) and the rest to the offices, including kitchen use and the humidification system.

In designing the new energy system, we have taken the current one as our base point and then expanded this using different technologies for energy production.

We have created designs for two representative periods: a Near Future (2025–2030) and a Mid-Century (2040–2050) time frame. As shown in Fig. 2, for each of these periods we have then defined three different scenarios for the design of the energy system: (1) Hydrogen-Electric; (2) All-Electric; and (3) Combined. Our motivation for considering these particular scenarios comes from first comparing the cost of energy in the two extreme cases, namely having a hydrogen grid connection only as in scenario 1 and an electricity grid connection only as in scenario 2. The third scenario, a combination of the first two and with both hydrogen and electricity grid connections, is then designed based on the resulting cost analyses.

In each of these scenarios, we use different production units depending on whether electricity or hydrogen is the main energy carrier. The sizes of the units are also different. Modelling is conducted from the demand side of the energy system. So the size of each component is obtained starting with electricity load, heat demand, etc. Our model

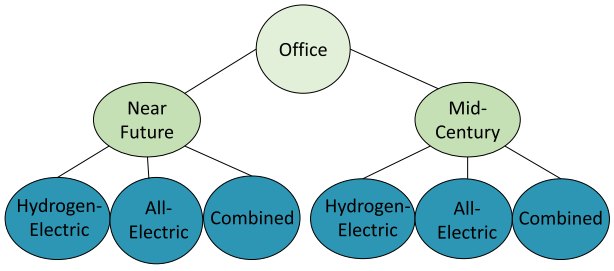

Fig. 2. Scenarios and representative years for our design analysis.

takes into account the building's entire supply chain, including production from wind and solar, storage necessities – both seasonal and daily – transport infrastructure, thermal demand, electricity demand and other end uses. For components outside of the physical location of the building, such as the wind turbines and external storage, we model and account for only precisely the capacity we need, obtained from a larger national supply network. As such, the inputs into our model are the demand profiles of different consumption units, solar and wind profiles and physical constraints of the production units, whilst its outputs are the size of each production unit, the supply profile and the system cost of energy.

4. Scenario analysis and results

In this section we present three different scenarios for the design of the STCA's energy system. For each we simulate the system as follows: (1) simulation of energy demand flows for one year, at 15-min intervals; (2) dimensioning of the wind turbine according to the wind profile and total energy requirements, after subtracting local solar production; (3) establishment of a dispatch priority sequence for components based on the requirements of each scenario (as mentioned under *main assumptions* in Section 4.1 and 4.2 and in the case descriptions in Section 4.3); (4) for every 15-min time step, solving the energy equation by balancing demand with the available generating components; (5) use of the external storage component, if there is a wind surplus or a supply deficit, to resolve the mismatch; and (6) calculation of the system costs, followed by the sensitivity analysis.

4.1. Hydrogen-electric scenario

4.1.1. System description

In the first scenario, we design a system with hydrogen as the main energy carrier.

As shown in Fig. 3, here the sole energy infrastructure is the hydrogen grid. It is assumed that this is a converted or retrofitted natural gas grid. Initial investigations indicate that it is indeed feasible to retrofit the existing natural gas infrastructure to create a hydrogen grid with minimal extra costs [29,30]. Hydrogen production is assumed to be centralized offshore, using the electricity from an offshore wind farm, and energy storage is also assumed to be centralized, using salt caverns. At the building, electricity is produced locally from solar panels on the roof and from a stationary fuel cell (SFC), which we assume to be a stacked system of cells of the kind also used in FCEVs. Heating is provided by a hydrogen-fuelled boiler, supplemented with heat extracted from the stationary fuel cell. Cooling is by an air-conditioning (AC) system. On the mobility side, we assume that one third of vehicles parking at the site are battery electric vehicles (BEVs) and two thirds are fuel cell electric vehicles (FCEVs). Both types can be charged and refuelled at the office

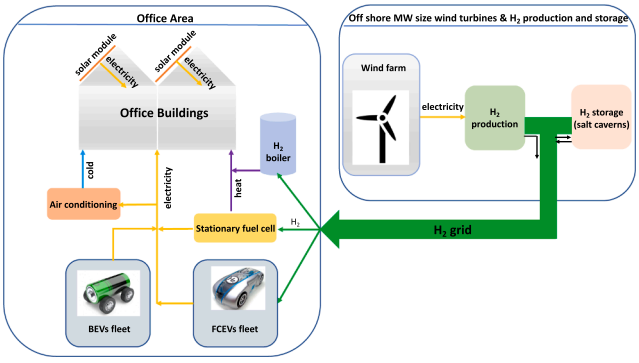

Fig. 3. Components of the energy system in Hydrogen-Electric scenario. The orange links show the electricity flow, the green links show the hydrogen flow, the purple link show the heat flow, and the blue link shows the cold flow.

location. The vehicles are used during peak load periods and at times of supply-demand mismatch when the solar panels and stationary fuel cell cannot meet the load demand. Note that hydrogen is used for the all lab and other activities where natural gas is currently used; for clarity, we do not show these hydrogen links in the figure.

The *main assumptions* in this scenario can be summarised as follows.

- Both FCEVs and BEVs deliver constant power of 10 kW to the grid in V2G mode, in order not to overheat the fuel cells and not to degrade the batteries too much.
- In V2G mode, FCEVs are connected directly to the hydrogen grid and so we do not use hydrogen from the tank for electricity production. As such, we include neither the refuelling regimes of FCEVs nor the installation costs of a hydrogen refuelling station in our cost analysis. The cost of hydrogen used from the grid is based on the cost calculation presented in Section 4.2.
- For BEVs, too, we do not take into account the charging pattern at the building. We assume that they arrive with a random level of charge between 50% and 100% and that we discharge them in V2G mode to no less than 20% of battery capacity, which is enough to drive about 100 km. The cost of the electricity used in V2G mode is assumed to be 0.25 €/kWh in Near Future and 0.15 €/kWh in Mid-Century (cf. Table A.10 in Appendix A).
- We do not consider the on-site production of hydrogen from excess solar energy, using a local electrolyser. This is due to the fact that, based on the size of the local solar generation system and the load profile at the STCA, it is rarely the case that there will be excess solar energy. So, any hydrogen produced in this way would be very expensive due to the low utilisation of the electrolyser.
- Electricity production is prioritised in the following order: solar, stationary fuel cell, FCEVs and finally BEVs. Note that solar and stationary fuel cell generation cover the base load, with electric vehicles used only during peak hours and periods of supply-demand mismatch.
- All current natural gas consumption is replaced by hydrogen.

Based on these assumptions, we have simulated the energy system in the Near Future and Mid-Century time frames with the main goal being to balance supply and demand at 15-min intervals. Figs. 4 and 5 show the annual energy balance for the two time frames, including the energy flows to and from each component in the system. As can be seen, in both cases about 32% of total energy comes from underground storage. Electricity generated from V2G-connected FCEVs is 2836 MWh/year in Near Future and 1812 MWh/year in Mid-Century. BEVs are rarely used, since we prioritize FCEVs. Fig. 6 shows the box plot for the number of EVs used for energy production over the course of one year. Frequently, up to 100 EVs are needed for balancing purposes in Near Future, and 50 in Mid-Century. Moreover, they are needed mainly between 4:00 and 18:00, with 4:00–6:00 being primarily when the system is starting up for the day and 7:00–18:00 being the office hours responsible for the bulk of energy consumption.

4.1.2. Techno-economic analysis

To obtain the system levelized cost of energy for the building, we first need to calculate the total system cost of energy (TSCoE) (cf. Eqs. (1)–(5)). As explained in Section 2.4, for TSCoE we need to calculate the total cost of each component in the energy system (cf. Eq. (2)) from its investment, operation and maintenance costs and its lifetime. In Appendix A, these values are presented for each component, for both the Near Future and the Mid-Century time frames, in Tables A.9 and A.10. Note that these tables contain all the various components used in all three scenarios.

Using these component costs and Eqs. (3)–(5), the total cost of each component – together with its size, capital cost and operation and maintenance costs – is calculated and presented in Appendix B Table B.11. The cost distribution bar plots for this scenario are presented in Appendix F Fig. F.20. The size of each component is chosen based on the building's demand profile. As we can see in that table, the size of the wind turbine is relatively large given the building's overall energy demand. This is due to all the energy losses involved in the conversions from electricity to hydrogen and vice versa. For the turbine, a capacity factor of 58.6% is obtained in the model. This is for the AC power coming from the turbine itself, before any transmission or conversion losses. The average efficiency of the electrolyser over a year using the higher heating value (HHV) of hydrogen is 77% (51.1 kWh/kg) is Near Future and 82% (47.9 kWh/kg) in Mid-Century. For simplicity, in the Mid-Century period these technical parameters are kept the same and future technological improvements are instead incorporated into cost parameters. In specifying the size of storage in salt caverns, we only take into account the quantity of hydrogen we need in the system.

Table 2 presents the (system) levelized cost of energy for each production unit and for the building's entire energy system using the total cost of each unit and the total energy it produces. All the hydrogen-related costs are based on the HHV of hydrogen. $SLCOE_e$ refers to the system levelized cost of electricity and $SLCOE_h$ the system levelized cost of heat for the entire energy system (given in €/kWh). $SLCOE_{H2}$ refers to the system levelized cost of hydrogen production taking into account production, storage, infrastructure and transportation costs (given in €/kg). Finally, $SLCOE_{Office}$ refers to the system levelized cost of energy (electricity, heat, gas) for the entire system and $SCOE_B$ the specific cost of energy for the building. As this table shows, the SLCoE for BEVs is one of the highest figures. This is due the high cost of bidirectional chargers and their low utilisation in the system. Since we use the same number of bidirectional chargers in both Near Future and Mid-Century, and because the utilisation of BEVs is even lower in the latter than in the former, the SLCoE of BEVs increases in the Mid-Century time frame.

4.1.3. Sensitivity analysis

The parameters for the mid Mid-Century time frame contain a higher level of uncertainty. For this period, therefore, a sensitivity analysis has been conducted for those parameters with a major impact on $SLCoE_{Office}$ or containing a high degree of uncertainty, such as wind turbine, cost of V2G infrastructure and WACC. Table 3 summarizes the parameters used in this analysis and the range of the value change for each of them. For most, we have added ±25% to the original investment cost or lifetime (cf. Table A.9 in Appendix A for nominal values). For WACC we have chosen 1% and 5% to study the effect of different discount rates on the SLCoE. The nominal value for WACC is 3%, as mentioned in Section 2.4.

The results of the sensitivity analysis are presented in Fig. 7. The vertical red line represents the original value. Percentages shown in the graph are the relative changes to the total system costs in response to the parameter deviations. Based on these results we can conclude that WACC, wind-turbine and hydrogen production costs have the greatest effect on the building's SLCOE.

4.2. All-Electric scenario

4.2.1. System description

In the second scenario, we design a system with electricity as the main energy carrier.

As shown in Fig. 8, here the sole energy infrastructure is the electricity grid, which is connected to an offshore wind farm. Further, we investigate two different energy storage systems in this scenario: a local one at the office area and a central one, as shown in Fig. 8, both using a large stationary battery system. Due to lab activities and the need for the incinerator at the STCA, in this case we still use hydrogen to cover the gas demand for incineration. Once again, hydrogen production is assumed to be centralized offshore, using the electricity from an offshore wind farm (for clarity, we do not show the hydrogen links in Fig. 8). Electricity is also produced locally, from solar panels on the roof. Heating and cooling are provided by a storage system using heat

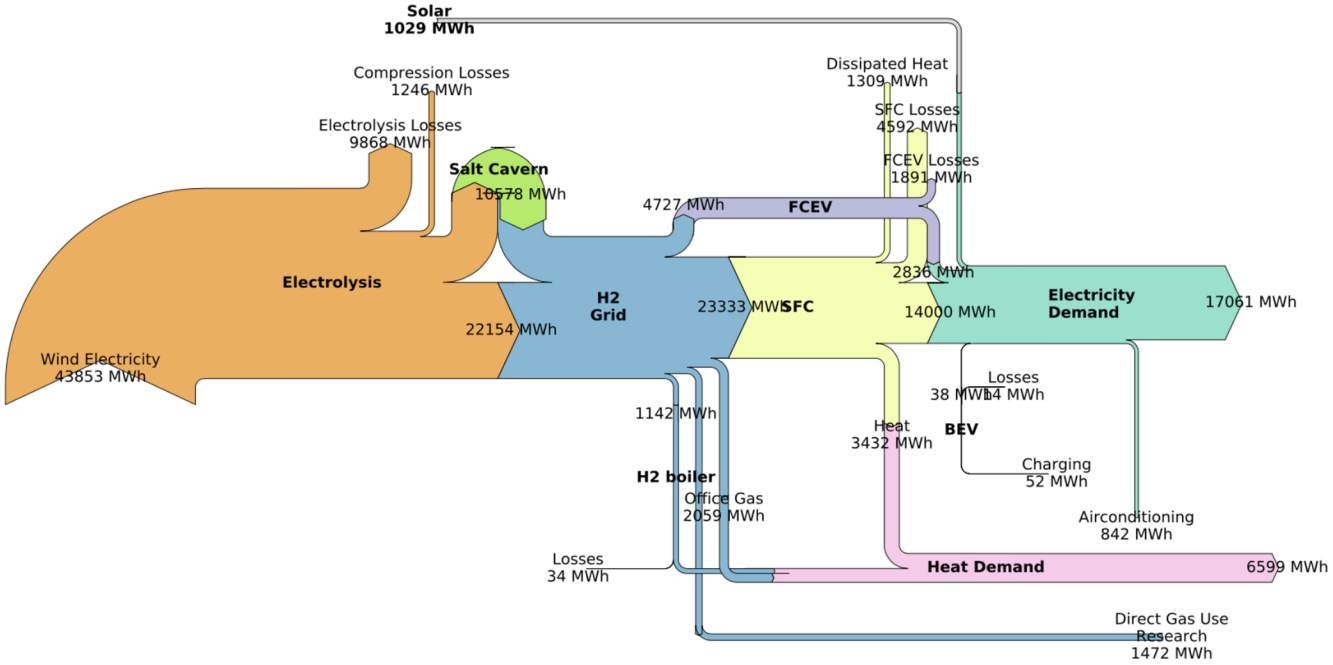

Fig. 4. Sankey diagram showing the annual energy balance for a fully renewable electricity, heating, and transport system at the office in near future for Hydrogen-Electric scenario.

pumps. On the mobility side, we assume that two thirds of vehicles parked at the site are BEVs, which can be charged at the office location, and one third are FCEVs, which are refuelled elsewhere. As in the previous scenario, both types of vehicles are used during peak load periods and at times of supply-demand mismatch when the solar panels and wind power cannot meet the load demand.

The *main assumptions* in this scenario can be summarised as follows.

- As in the previous scenario, both FCEVs and BEVs deliver constant power of 10 kW to the grid in V2G mode.
- In V2G mode, FCEVs draw hydrogen directly from their tanks for electricity production. We make sure that there is always 1 kg of hydrogen left in the tank, which is enough to drive about 100 km. As such, we include neither the refuelling regimes of FCEVs nor driving patterns in our cost analysis. The cost of the hydrogen used from the cars in V2G mode is assumed to be 6 €/kg in Near Future and 4 €/kg in Mid-Century (cf. Table A.10 in Appendix A) and they refuel outside of the office.
- BEVs are charged by excess wind energy from the electricity grid and discharged in V2G mode to no less than 20% of battery capacity,

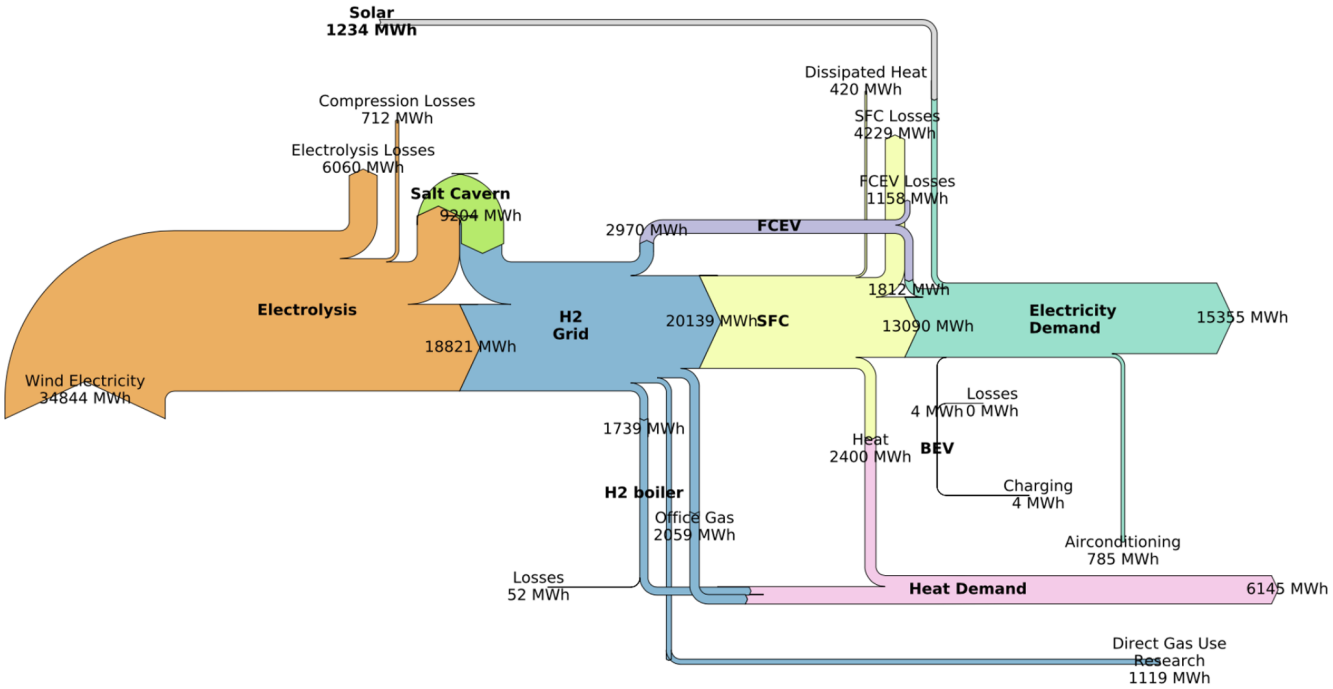

Fig. 5. Sankey diagram showing the annual energy balance for a fully renewable electricity, heating, and transport system at the office in mid-century for Hydrogen-Electric scenario.

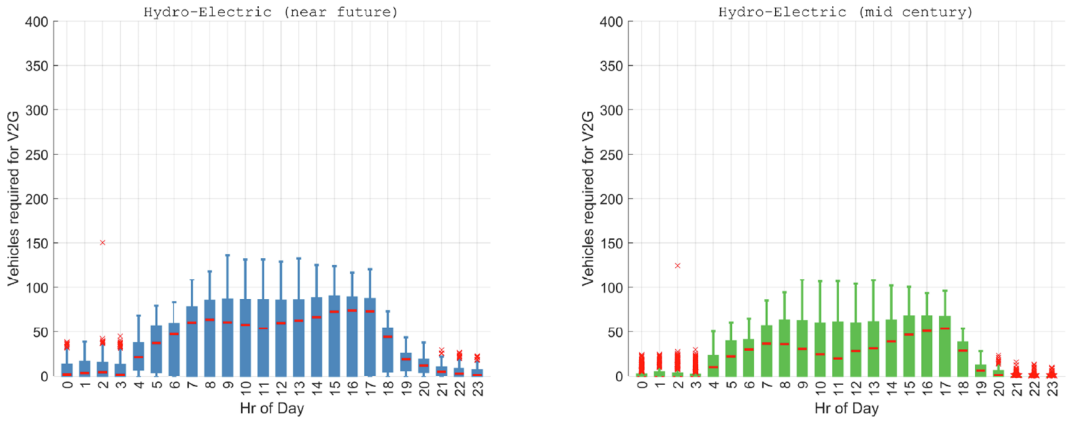

Fig. 6. Number of vehicles required and used in V2G-mode for Hydrogen-Electric scenario in near future and mid-century. Central red mark indicates the median, the bottom and top edges of the box indicate the 25th and 75th percentiles, respectively. The whiskers go up to extreme data points not considered outliers. The red markers are individual outliers.

Table 2
Cost analysis for Hydrogen-Electric scenarios in near future and mid-century.

(System) levelized cost of energy	Near Future	Mid-Century
$LCOE_{Solar}$ [€/kWh]	0.07	0.03
$LCOE_{Wind}$ [€/kWh]	0.04	0.02
$SLCOE_{H2}$ [€/kg]	3.12	1.90
$SLCOE_{BEV}$ [€/kWh]	1.14	5.36
$SLCOE_{FCEV}$ [€/kWh]	0.25	0.13
$SLCOE_{SFC}$ [€/kWh]	0.14	0.08
$LCOE_{e}$ [€/kWh]	0.16	0.08
$SLCOE_{h}$ [€/kWh]	0.04	0.03
$SLCOE_{Office}$ [€/kWh]	**0.117**	**0.062**
$SCOE_{B}$ [€/ m^2/year]	30.31	14.73

which is enough to drive about 100 km. The use of an 80% range is also intended to reduce battery degradation. The cost of the energy used in V2G mode is based on the cost calculations for the electricity grid in Section 5.2.

- Electricity production is prioritized in the following order: solar and wind, BEVs, stationary battery system and finally FCEVs. Note that solar and wind primarily cover the base load, with electric vehicles and the stationary battery used only during peak hours and periods of supply-demand mismatch.
- All current natural gas consumption by the lab is replaced with hydrogen, and the rest (e.g. kitchen use) superseded by electric options.

Based on these assumptions, we have simulated the energy system with the main goal being to balance supply and demand at 15-min intervals. Figs. 9 and 10 show the total energy produced over an entire year with a central storage system in the Near Future and Mid-Century time frames, respectively. As can be seen, in this scenario between 26% and 31% of total energy comes from storage (both battery and salt caverns). In Near Future, electricity generated from V2G-connected BEVs is 1898 MWh/year and from FCEVs it is 1315 MWh/year. In the Mid-Century time frame, those figures are 3511 MWh/year from BEVs and 798 MWh/year from FCEVs. As we can see, BEVs are used more frequently here than in the previous scenario as they are prioritized for energy production in this case. Since there is a limit on the battery's state of charge, however, FCEVs are also used quite often.

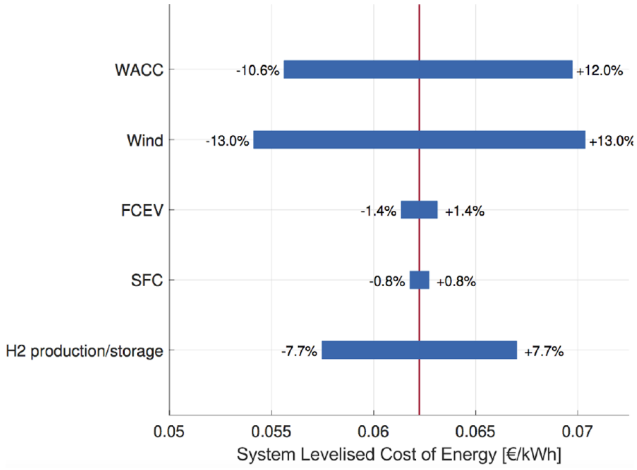

Fig. 7. Sensitivity analysis for Hydrogen-Electric scenario in mid-century.

Fig. 11 shows the box plot for the number of EVs used for energy production over the course of one year. As we can see, the average number needed for balancing purposes is below 50 in Near Future and below 70 in Mid-Century. Due to the storage capacity limitations of the BEVs and the stationary battery, however, in this scenario FCEVs are used more often during peak hours and that results in more outliers both time frames. Moreover, the cars are needed mainly between 7:00 and 19:00, i.e. during the office hours responsible for the bulk of energy consumption.

Table 3
The input parameters altered for the sensitivity analysis per sensitivity parameter chosen. IC stands for Investment Costs and LT for lifetime.

Sensitivity Parameter	Contents	Values tested
SFC	IC of SFC.	±25%
H2 production and storage	Salt Cavern [€/kg H_2 stored]. IC of: Electrolyzer, water purification and pure water tank.	±25%
FCEV	IC of: FCEV and Discharge infrastructure.	±25%
BEV	IC of: BEV and bi-directional chargers.	±25%
Stationary Battery	IC of: BESS and External Storage.	±25%
Battery Lifetime	LT of: BEV, BESS and External Storage.	±25%
Wind	IC of wind turbine.	±25%
WACC	WACC (= discount rate)	{1%, 5%}

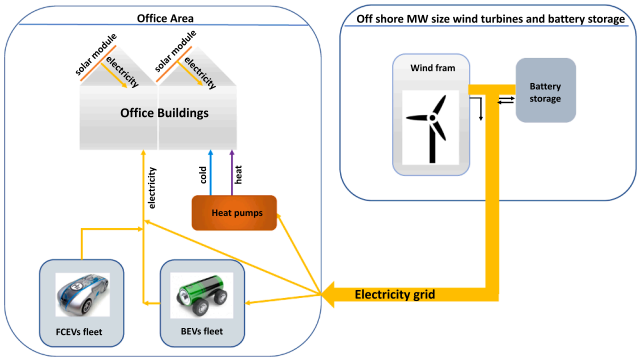

Fig. 8. Components of the energy system in All-Electric scenario. The orange links show the electricity flow, the purple link show the heat flow, and the blue link shows the cold flow.

4.2.2. Techno-economic analysis

To obtain the system levelized cost of energy for the building in this scenario, we follow similar steps as in the previous one to first calculate the TSCoE. The investment, operation and maintenance costs and the lifetime of each unit in the energy system are presented in Appendix A Table A.9, whilst the cost distribution bar plots for this scenario are presented in Appendix F Fig. F.21.

Using these component costs and Eqs. (3)–(5), we now calculate the total cost of each component. In this scenario, to specify the size of storage we consider two cases. In the first case, all the energy is stored locally in a very large battery system. Despite its substantial capacity, however, over the course of a year there will still be many hours during which it is full, and we are therefore unable to store excess energy. In such situations we would have dispose of that energy by, for example, giving it to the neighbourhood. There are also many hours when the battery is empty but there is no excess energy to charge it, and so we have to assume that we will need to buy more expensive electricity from an external source. In the second case we still have a local stationary battery with a capacity of 12 MWh to provide backup power, but the bulk of storage occurs centrally in a large stationary battery at the wind farm. As in the previous scenario with salt caverns, here also we only consider the storage cost for the amount of energy we actually draw from this central storage facility. We also use the same efficiency data for the wind turbine and electrolyser as in the previous scenario.

The total cost of each component, together with its size, capital cost and operation and maintenance costs, is presented in Appendix C Table C.12 for external primary storage and in Table C.13 for storage in a large local battery. As we can see, in this All-Electric scenario the size of the wind turbine is much smaller than in the Hydrogen-Electric scenario since here we do not have any energy conversion and so far less is lost. Another important figure in this scenario is the cost of storage in each of the two cases. Based on these, it is again more economical to store energy centrally in the All-Electric scenario. Our calculation of the system levelized cost of energy is therefore derived from that situation.

Table 4 presents the (system) levelized cost of energy for each production unit and for the building's entire energy system based on external storage and using the total cost of and the total energy produced by each unit. Since BEVs are used more often in this scenario, $SLCOE_{BEV}$ is much lower than in the previous one (cf. Table 2).

4.2.3. Sensitivity analysis

The results of the sensitivity analysis for the All-Electric scenario in the Mid-Century time frame, based on the variation of the parameters in Table 3, are shown in Fig. 12.

In this case, WACC and the cost of wind turbine have the greatest effect on the system levelized cost of energy in Mid-Century; the other parameters have more or less similar effects in changing the $SLCoE_{Office}$.

4.3. Combined scenario

4.3.1. System description

From the techno-economic analyses of scenarios 1 and 2, it is clear that both are extreme situations with a number of advantages and disadvantages. For our last scenario, therefore, we designed a combined situation with both electricity and hydrogen grid connections. Our goal is to compare its total system cost and the system levelized cost of energy with scenarios 1 and 2. There are several possible design choices in this case, depending on the purpose of the system; more local production and less import from external grids, for instance, or lower

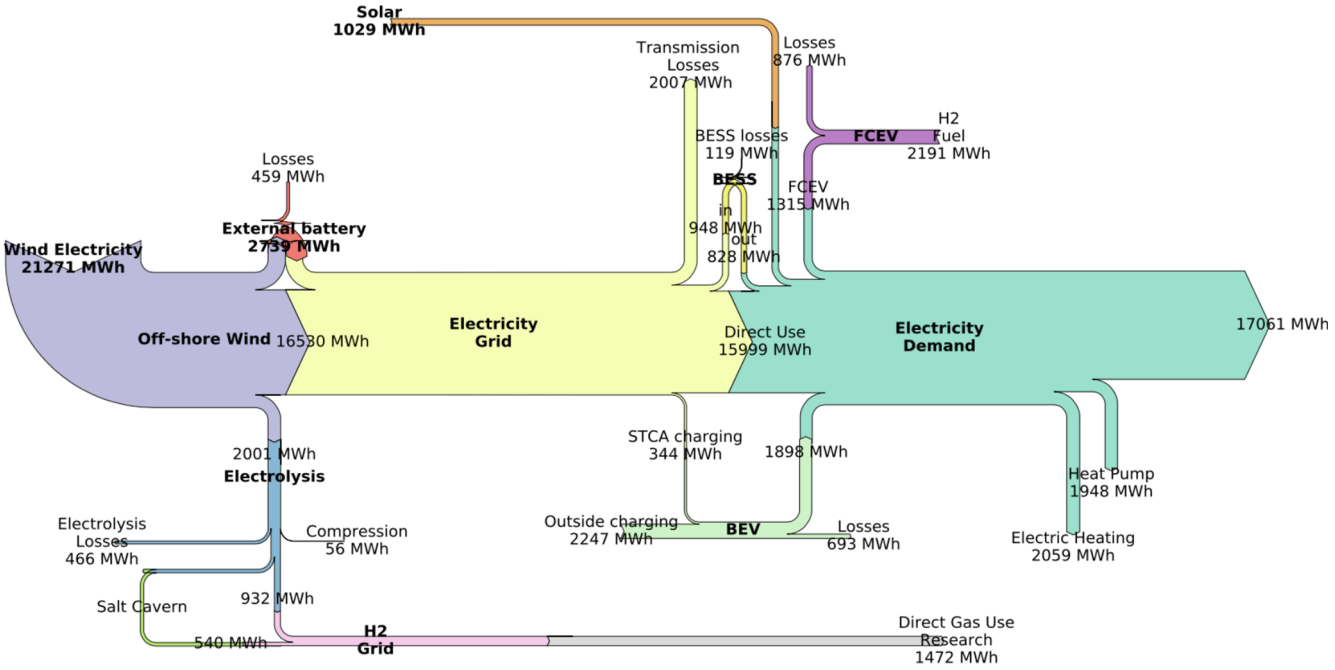

Fig. 9. Sankey diagram showing the annual energy balance for a fully renewable electricity, heating, and transport system at the office in near future for All-Electric scenario.

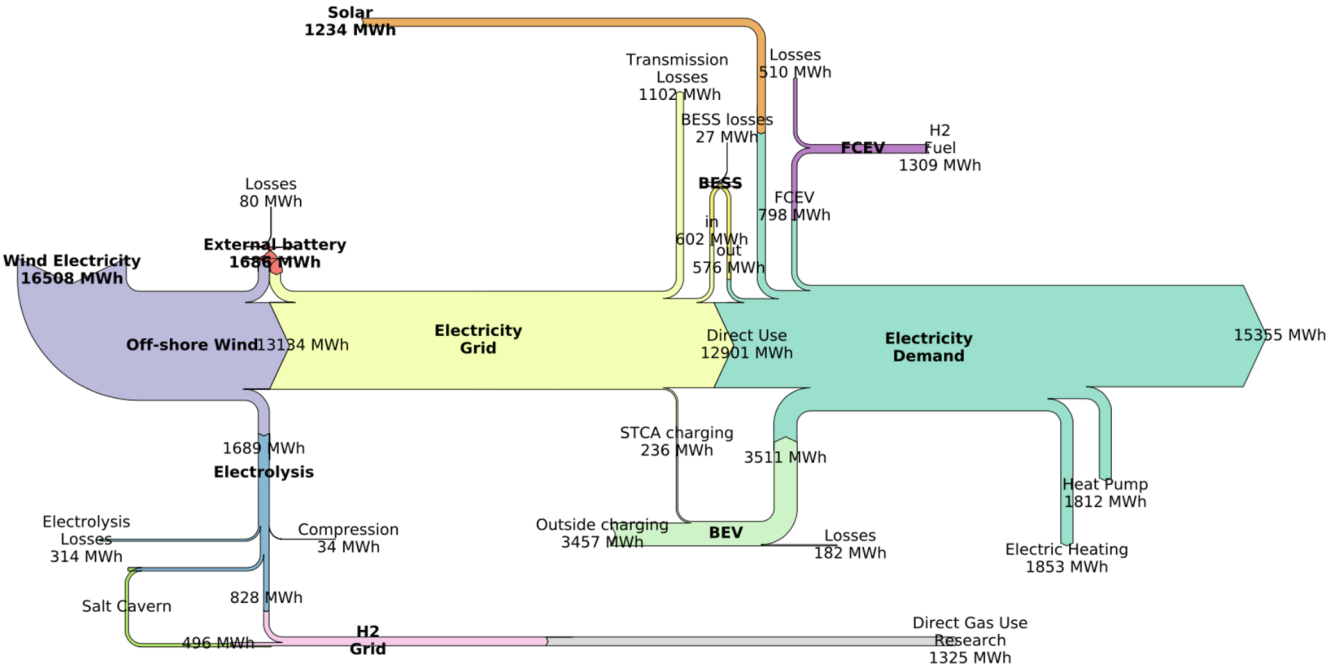

Fig. 10. Sankey diagram showing the annual energy balance for a fully renewable electricity, heating, and transport system at the office in mid-century for All-Electric scenario.

energy costs. We can thus pick different components and different priorities for the source of energy production. In the end, we selected three cases for consideration in this scenario: Case (1) a combined situation with heat pumps; Case (2) a combined situation with a boiler; and Case (3) a combined situation using fixed costs for both electricity and hydrogen grids. Each of these cases is described below.

Case 1. The energy system for this combined situation is shown in Fig. 13. As infrastructure, we have both the electricity grid and the hydrogen grid. Both forms of energy are produced offshore by a wind turbine, and for storage we use salt caverns. Electricity is also produced locally from solar panels on the roof and from a stationary fuel cell. For heating and cooling, we use heat pumps. On the mobility side, half of the cars are BEVs and the other half are FCEVs, and as in the other scenarios we do not take into account their refuelling or recharging patterns. The FCEVs are connected to hydrogen grid in V2G mode and so we use the cost of hydrogen bought from the grid. The cost of electricity delivered to the grid by BEVs in V2G mode is taken from Table A.10 in Appendix A. Note that hydrogen is used for the all lab and other activities where natural gas is currently used; for clarity, we do

Table 4
Cost analysis for All-Electric scenarios with central main storage in near future and mid-century.

(System) levelized cost of energy	Near Future	Mid-Century
$LCOE_{Solar}$ [€/kWh]	0.07	0.03
$LCOE_{Wind}$ [€/kWh]	0.04	0.02
$SLCOE_{Wind}$ [€/kWh]	0.07	0.05
$SLCOE_{H2}$ [€/kg]	3.66	2.38
$SLCOE_{BEV}$ [€/kWh]	0.50	0.22
$SLCOE_{FCEV}$ [€/kWh]	0.40	0.26
$SLCOE_{BESS}$ [€/kWh]	0.61	0.35
$SLCOE_{e}$ [€/kWh]	0.15	0.1
$SLCOE_{h}$ [€/kWh]	0.06	0.05
$SLCOE_{Office}$ [€/kWh]	**0.123**	**0.080**
$SCOE_{B}$ [€/ m^2/year]	31.82	18.88

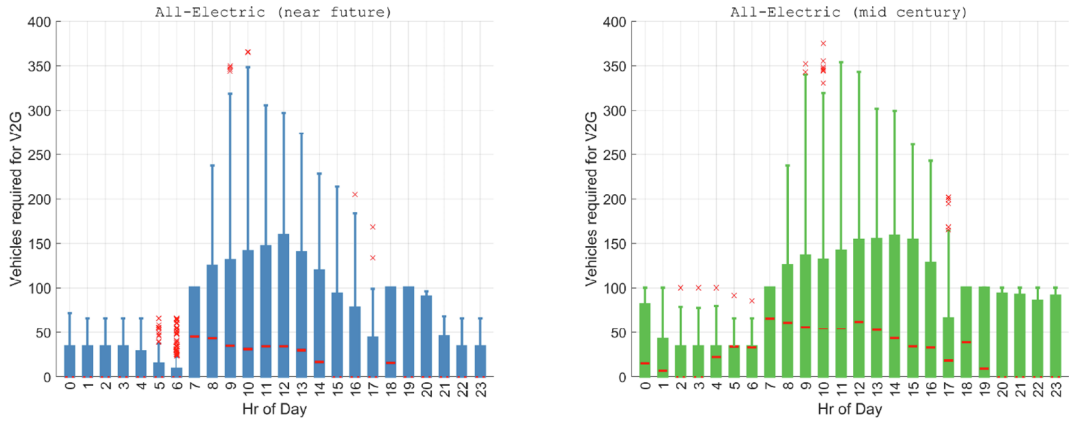

Fig. 11. Number of vehicles required and used in V2G-mode for All-Electric scenario in near future and mid-century. Central red mark indicates the median, the bottom and top edges of the box indicate the 25th and 75th percentiles, respectively. The whiskers go up to extreme data points not considered outliers. The red markers are individual outliers.

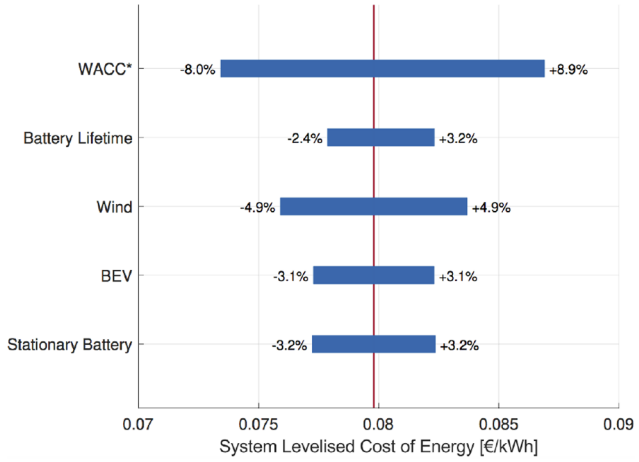

Fig. 12. Sensitivity analysis for All-Electric scenario in mid-century.

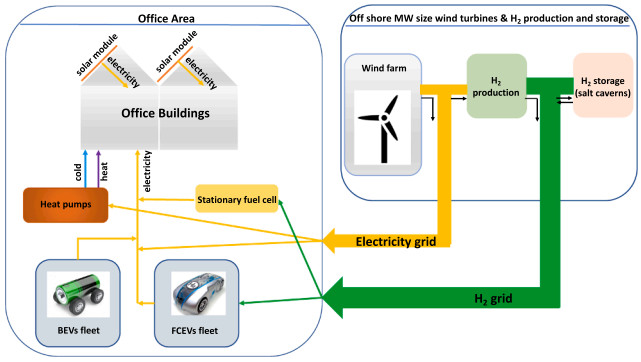

Fig. 13. Components of the energy system in Combined scenario Case 1 using heat pumps. The orange links show the electricity flow, the green links show the hydrogen flow, the purple link show the heat flow, and the blue link shows the cold flow.

not show these hydrogen links in the figure. The order of production in this case is solar and wind first, then stationary fuel cell, then FCEVs and finally BEVs.

Case 2. The energy system for this combined situation is shown in Fig. 14. The system design and components in this case are the same as in the previous one, except for heating and cooling. Instead of heat pumps, here we use a hydrogen-fuelled boiler and the collected heat from the stationary fuel cell to cover the demand for heat, whilst for cooling we use an air-conditioning system. The order of electricity production is the same as in Case 1.

Case 3. This has the same setup as Case 1, but we do not design the wind turbine based on the demand profile or take into account storage. Instead, we use fixed costs for both energy carriers. For electricity, the cost is chosen based on the $SLCoE_{Wind}$ obtained from the techno-economic analysis in Section 4.2, i.e. 0.068/kWh in the Near Future time frame and 0.047 €/kWh in Mid-Century. For hydrogen it is chosen based on the $SLCoE_{H2}$ obtained from the techno-economic analysis in Section 4.1, i.e. 3117 €/kg in Near Future and 1901 €/kg in Mid-Century. The order of energy production is similar to that in Case 1, except that here we use the solar and wind power to cover two thirds of the base load and the stationary fuel cell to cover the other one third. Moreover, we collect and use the heat from the stationary fuel cell. The rest of the demand for heat is met by the heat pumps.

As the results obtained in all three cases are similar, for brevity here we present only those from Case 1. The annual energy distribution for the building in this case is shown in Appendix E Figs. E.18 and E.19. In all three cases in the Combined scenario, about 24% of total energy used comes from storage. Moreover, since we use both electricity and

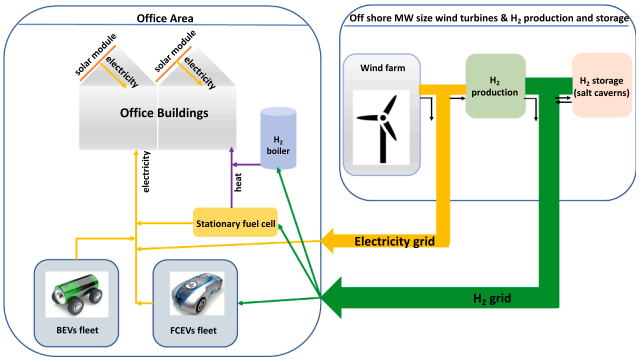

Fig. 14. Components of the energy system in Combined scenario Case 2 using a boiler. The orange links show the electricity flow, the green links show the hydrogen flow, the purple links show the heat flow, and the blue link shows the cold flow.

hydrogen grids, the use of electric vehicles differs quite substantially from that in either the Hydrogen-Electric or the All-Electric scenario. As shown in Fig. 15, here we use both types of EVs much less frequently. The reason for this is that they are needed much less, due to the availability of power from both the electricity grid and the stationary fuel cell. As this pattern is very similar in all three cases in the Combined scenario, we present only the results of Case 1.

4.3.2. Techno-economic analysis

The total costs of components for each of the three cases are presented in Appendix D, in Tables D.14–D.16. The cost distribution bar plots for Case 1 are shown in Appendix F Fig. F.22; we omit the other two for brevity, as their results are similar. Since we here use both grids and include both electricity and hydrogen-based units, the capacity and hence the cost of each unit is different from those reported in the Hydrogen-Electric and All-Electric scenarios.

The results of the techno-economic analyses of these three cases are presented in the tables below. As we can see in Tables 5 and 6, using the heat pumps or the boiler does not change the $SLCoE_{STCA}$ much. Table 7 shows that using the fixed-grid cost also results in similar system levelized costs of energy as in the other two combined cases.

The sensitivity analyses for the different cases in the Combined scenario shows that the effect of cost variations of different components on the system levelized cost of energy is similar to those in scenarios 1 and 2. Consequently, those results are not presented in this section.

4.4. Summary of the results

Table 8 summarises main results obtained from analysing the three scenarios. The first important result is the significant role of storage in this energy system, since it accounts for between 20% and 30% of the supplied energy. Our results also show that using salt caverns and hydrogen for energy storage is much cheaper than using large battery storage systems. Hence, despite using the external storage option in the All-Electric scenario, its $SLCoE_{Office}$ is still higher than in the Hydrogen-Electric scenario due to higher storage costs. Note that the wind turbine capacity factor is a crucial determinant of the economic results and a lower capacity factor is linked to a higher levelized cost of wind energy. However, this research compares costs between different scenarios, focusing on balancing and storage using various alternatives. Note that the wind energy costs are equal across the scenarios and the size of the wind turbine is the only changing factor depending on the energy demand in each scenario. Thus, while these costs are a significant factor in the total $SLCoE_{Office}$, they have a marginal effect on the relative evaluation of $SLCoE_{Office}$ of each scenario and do not impact the conclusions of the research, which is aiming to compare energy carrier alternatives and energy storage options.

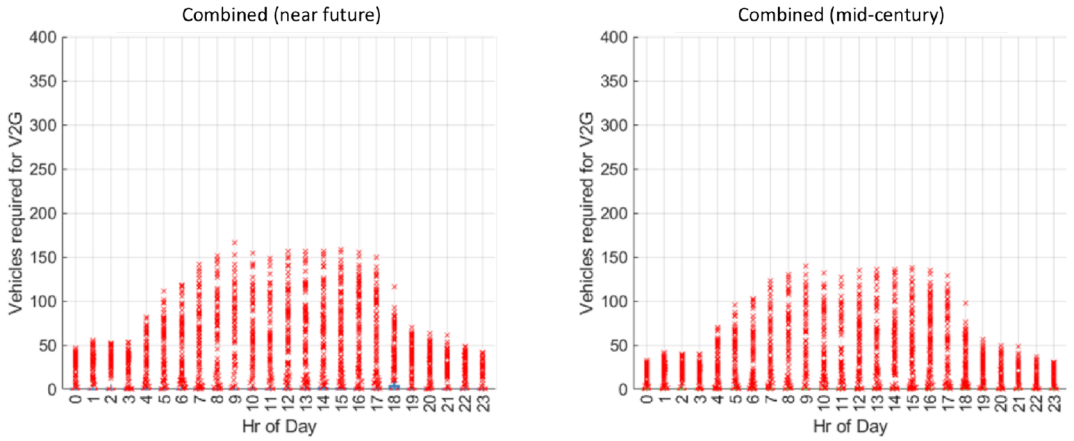

Fig. 15. Number of vehicles required and used in V2G-mode for Combined scenario Case 1 in near future and mid-century. Central red mark indicates the median, the bottom and top edges of the box indicate the 25th and 75th percentiles, respectively. The whiskers go up to extreme data points not considered outliers. The red markers are individual outliers.

Table 5
System Levelized Cost end results for Combined scenario Case 1 in Near-Future and Mid-Century.

(System) levelized cost of energy	Near Future	Mid-Century
$LCOE_{Solar}$ [€/kWh]	0.07	0.03
$LCOE_{Wind}$ [€/kWh]	0.04	0.02
$SLCOE_{Wind}$ [€/kWh]	0.06	0.04
$SLCOE_{H2}$ [€/kg]	4.34	2.58
$SLCOE_{BEV}$ [€/kWh]	1.4	1.27
$SLCOE_{FCEV}$ [€/kWh]	0.35	0.19
$SLCOE_{SFC}$ [€/kWh]	0.22	0.11
$SLCOE_{e}$ [€/kWh]	0.11	0.07
$SLCOE_{h}$ [€/kWh]	0.04	0.03
$SLCOE_{Office}$ [€/kWh]	**0.086**	**0.054**
$SCOE_{B}$ [€/m^2/year]	22.4	12.7

Table 6
System Levelized Cost end results for Combined scenario Case 2 in Near-Future and Mid-Century.

(System) levelized cost of energy	Near Future	Mid-Century
$LCOE_{Solar}$ [€/kWh]	0.07	0.03
$LCOE_{Wind}$ [€/kWh]	0.04	0.02
$SLCOE_{Wind}$ [€/kWh]	0.06	0.04
$SLCOE_{H2}$ [€/kg]	4.00	2.45
$SLCOE_{BEV}$ [€/kWh]	1.37	1.02
$SLCOE_{FCEV}$ [€/kWh]	0.35	0.18
$SLCOE_{SFC}$ [€/kWh]	0.21	0.11
$SLCOE_{e}$ [€/kWh]	0.10	0.06
$SLCOE_{h}$ [€/kWh]	0.07	0.04
$SLCOE_{Office}$ [€/kWh]	**0.087**	**0.056**
$SCOE_{B}$ [€/ m^2/year]	22.6	13.2

The other interesting aspect is the system's utilisation of EVs, especially the fact that, in the Hydrogen-Electric scenario, fewer are used in the Mid-Century time frame than in Near Future. And that the reverse is the case in the All-Electric scenario. This is, of course, the result of the system configuration and the order in which the production units are used. The decrease in the utilisation of EVs in the Hydrogen-Electric scenario can be explained by decreasing demand for electricity in Mid-Century, whilst the solar and stationary fuel-cell components have by then become more efficient. The increase in the use of EVs in the All-Electric scenario in Mid-Century may appear counterintuitive at first sight, but can be explained as follows: as solar and wind are intermittent sources of energy, BEVs are employed more often as a back-up; and since BEV parameters such as battery capacity and conversion efficiency are

Table 7
System Levelized Cost end results for Combined scenario Case 3 in Near-Future and Mid-Centuryẋmllabelt0035

(System) levelized cost of energy	Near Future	Mid-Century
$LCOE_{Solar}$ [€/kWh]	0.07	0.03
$SLCOE_{Wind}$ [€/kWh]	0.07	0.05
$SLCOE_{H2}$ [€/kg]	3.12	1.90
$SLCOE_{BEV}$ [€/kWh]	1.26	1.06
$SLCOE_{FCEV}$ [€/kWh]	0.29	0.15
$SLCOE_{SFC}$ [€/kWh]	0.14	0.08
$SLCOE_{e}$ [€/kWh]	0.13	0.07
$SLCOE_{h}$ [€/kWh]	0.02	0.01
$SLCOE_{Office}$ [€/kWh]	**0.08**	**0.042**
$SCOE_{B}$ [€/m^2/year]	27.3	13.8

improved in Mid-Century, greater use of EVs is facilitated. Moreover, the sparse utilisation of BEVs in the Hydrogen-Electric scenario means that almost all the stored energy comes from salt caverns. In the All-Electric scenario, since more BEVs are used in Mid-Century their share of storage is higher than in the Near Future period.

Finally, the results from the Combined scenario confirm our hypothesis that, if we use both electricity and hydrogen in the building's energy system, and different production units and storage options, our energy system is not only more flexible but also more economic. We also see that in all these cases the number of cars operating in V2G mode is quite small by comparison with the total parking capacity of the building. This shows the feasibility of V2G application at such office blocks.

5. Optimal scheduling

The operational management of an energy system is an important aspect of its performance and so needs to be considered alongside its design. In this section, therefore, we focus on the operational level and provide an optimal scheduling for the deployment of production units in the energy system, with the view to using them – and especially EVs – in a more systematic and efficient way and to minimising production costs.

5.1. System model and constraints

The setup of the energy system considered for this aspect of our study is equivalent to the one in Case 1 of the Combined scenario and is presented in Fig. 13. Electricity can either be produced using local units such as solar panels and stationary fuel cells or be drawn from the external electricity grid, which is connected to an offshore wind farm. Moreover, both BEVs and FCEVs are used for load balancing during

Table 8
Summary of the results for the scenario analysis.

	Hydrogen-Electric		All-Electric		Combined- Case 1	
Item	Near Future	Mid-Century	Near Future	Mid-Century	Near Future	Mid-Century
Total Energy Supply [MWh/year]	32,770	28,029	23,610	20,217	26,093	22,529
Total Storage (%)	32	32	26	31	24	24
– Hydrogen (%)	32	32	7	6	24	24
– Electricity (%)	0	0	19	25	0	0
Average # of EVs	100	50	50	70	10–20	10–20
Energy production BEV [MWh/year]	38	4	1898	3511	61	31
Energy production FCEV [MWh/year]	2836	1812	1315	798	827	613
$SLCOE_{Office}$ [€/kWh]	0.117	0.062	0.123	0.080	0.086	0.054
$SCOE_B$ [€/ m^2/year]	30.31	14.73	31.82	18.88	22.4	12.7

peak hours and periods of mismatch between supply and demand. Heating is provided by heat from the stationary fuel cell and by heat pumps. Cooling, too, is provided by the heat pumps. We also have the hydrogen grid, which delivers hydrogen to both the stationary fuel cell and FCEVs. The objective of the system is to use production units more systematically and to minimise the cost of energy production based on the cost of fuel and operation and maintenance costs for each of the controllable production units, i.e. stationary fuel cells and EVs. Moreover, we endeavour to minimise degradation of the stationary fuel cell and of BEVs and FCEVs in V2G mode.

Here, the states of the system are the operating state of the stationary fuel cell, operating states of FCEVs and BEVs and the state of charge of BEVs. We model the system in discrete time and the state equations can be defined as

$$\nu_{SFC}(k) = \nu_{SFC}(k-1) + \delta^{\text{start}}_{SFC}(k) - \delta^{\text{stop}}_{SFC}(k) \tag{10}$$

$$\nu_{f,i}(k) = \nu_{f,i}(k-1) + \delta^{\text{start}}_{f,i}(k) - \delta^{\text{stop}}_{f,i}(k) \tag{11}$$

$$\nu_{b,j}(k) = \nu_{b,j}(k-1) + \delta^{\text{start}}_{b,j}(k) - \delta^{\text{stop}}_{b,j}(k) \tag{12}$$

$$\nu_{SoC,j}(k) = \nu_{SoC,j}(k-1) - u_{b,j}(k)\eta_{dis}\Delta t \tag{13}$$

where $\nu_{SFC} \in \{0, 1\}$ is the operating state of the stationary fuel cell at time step k, $\nu_{f,i} \in \{0, 1\}$, $i = 1, ..., n_f$ is the operating state of the i-th FCEV at time step k, $\nu_{b,j} \in \{0, 1\}$, $j = 1, ..., n_b$ is the operating state of the j-th BEV at time step k, and $\nu_{SoC,j} \in \mathbb{R}$ is the state of charge of the battery of the j-th BEV at time step k. In the state equations, we also have the control variables to turn the units on and off, defined as $\delta^{\text{start}}_{pu}(k) = 1$ if production unit pu (stationary fuel cell, FCEV, or BEV) is started for power production at time step k and $\delta^{\text{start}}_{pu}(k) = 0$ otherwise. Similarly, $\delta^{\text{stop}}_{pu}(k) = 1$ if production unit pu (stationary fuel cell, FCEV, or BEV) is shut down at time step k and $\delta^{\text{start}}_{pu}(k) = 0$ otherwise. Moreover, $u_{b,j}(k)$ controls the amount of power produced by the j-th BEV at time step k, Δt is the size of the time step, and η_{dis} is the discharge efficiency of a BEV in the V2G mode. Note that the production units FCEV and BEV have n_f and n_b components, respectively. As well as the abovementioned control variables, we also control the amount of power bought from the electricity grid, $P_{e,grid}$, the amount of power produced by the stationary fuel cell, u_{SFC} and the amount of power produced by FCEVs, $u_{f,i}$.

In this model, we also include different operational constraints. One of these is related to the production capacity of each production unit pu (stationary fuel cell, FCEV or BEV) and its components at each time step k, which can be written as

$$\underline{U}_{pu}\nu_{pu}(k) \leqslant u_{pu}(k) \leqslant \bar{U}_{pu}\nu_{pu}(k), \tag{14}$$

taking into account the operating state of each unit at time state k defined in (11)–(10). Here $\underline{U}_{pu}$ indicates the possible minimum power production of each unit and $\bar{U}_{pu}$ the possible maximum power. Moreover, there is an upper threshold for the power we can buy from the electricity grid, $\bar{U}_{e,grid}$, which is equal to the wind power generated at time step k. This constraint is defined as

$$P_{e,grid} \leqslant \bar{U}_{e,grid}. \tag{15}$$

In order to make sure that no component of a production unit is switched on and off at the same time, the following constraint is used,

$$\delta^{\text{start}}_{pu}(k) + \delta^{\text{stop}}_{pu}(k) \leqslant 1. \tag{16}$$

As mentioned before, keeping the balance between supply and demand at each time step k is one of the main goals in the system. To satisfy this balance, we include the following constraint at each time step k,

$$P_D(k) = P_{solar}(k) + P_{e,grid}(k) + u_{SFC}(k) + \sum_{i=1}^{n_f} u_{f,i} + \sum_{j=1}^{n_b} u_{b,i}, \tag{17}$$

where $P_D(k) = P_{\text{load}}(k) + P_{\text{HP}}(k)$ is the power demand of the office at time step k including the load P_{load} and heat pumps demand P_{HP}, $P_{solar}(k)$ is the power production of the solar panels system at time step k, n_f indicates the number of FCEVs and n_b indicates the number of BEVs present at the energy system.

In addition to these constraints, we have included two others related to the fair use of electric vehicles. Using EVs in the V2G mode increases degradation of the battery and fuel cell. To be fair on their owners, therefore, we only use each EV in V2G mode for few hours at a time and we make sure that it is not used again for a certain period thereafter. These values can be defined based on the system requirements and the availability of cars. For the first constraint, we make sure that FCEVs are switched off after being used for T hours,

$$(1 - \delta^{stop}_{f,i}(k))\left(T - \sum_{t=k-T+1}^{k-1} \nu_{f,i}(t) + \nu_{f,i}(k)\right). \tag{18}$$

The same constraint holds for BEVs. For the second constraint, we keep the vehicle off for the next T' hours once it has been used in the V2G mode; i.e. at each time step k, the following must hold for each FCEV,

$$\sum_{t=k-T'+1}^{k-1} \delta^{stop}_{f,i}(t) + \delta^{stop}_{f,i}(k) \leqslant 1 - \nu_{f,i}(k), \tag{19}$$

and the same constraint holds for BEVs.

Finally, to minimise electricity consumption by heat pumps, we first use the heat extracted from the stationary fuel cell. The remainder of the demand for heat is then covered by the heat pumps; i.e.

$$H_{HP}(k) = \begin{cases} H_D(k) - H_{SFC}(k) & \text{if } H_D(k) \geqslant H_{SFC}(k) \\ 0 & \text{otherwise.} \end{cases} \tag{20}$$

Here, $H_D(k)$ is the demand for heat at time step k and $H_{SFC}(k) = u_{SFC}(k)\cdot\eta_H/\eta_e$ is the extracted heat from the stationary fuel cell at time step k, with η_H the efficiency of the fuel cell based on the HHV for the heat production and η_e its efficiency for electricity production. As mentioned before, the demand for heat includes the electricity demanded by the heat pumps for heating and cooling. The electricity demand of the heat pumps at time step k can be written as

$$P_{HP}(k) = H_{HP}(k)\cdot\frac{1}{COP_{month}} + C_{HP}(k)\cdot\frac{1}{COP_{month}}, \tag{21}$$

where $\mathrm{COP}_{\mathrm{month}}$ is the coefficient of performance of the heat pump for each month of the year and C_{HP} is the cooling production of the heat pump. Using Eqs. (20) and (21), the power demand in Eq. (17) can be adjusted.

In order to obtain a linear system with continuous and binary variables, we apply the mixed logical dynamical (MLD) formalism, which allows the transformation of logical statements involving continuous variables into mixed-integer linear inequalities. We apply the following equivalences [31] to transform the nonlinear constraints into linear ones:

$$[f(x(k)) \leqslant 0] \leftrightarrow [\delta(k) = 1] \text{ iff } \begin{cases} f(x(k)) \leqslant M(1-\delta(k)) \\ f(x(k)) \geqslant \varepsilon + (m-\varepsilon)\delta(k) \end{cases}$$
$$z(k) = \delta(k) f(x(k)) \text{ iff } \begin{cases} z(k) \leqslant M\delta(k) \\ z(k) \geqslant m\delta(k) \\ z(k) \leqslant f(x(k)) - m(1-\delta(k)) \\ z(k) \geqslant f(x(k)) - M(1-\delta(k)) \end{cases} \tag{22}$$

where M, $m \in \mathbb{R}$ are the upper and lower bounds on the linear function $f(x(k))$ and ε is the machine precision.

Based on the equivalence relations (22), the MLD model of (18) and (20) can be obtained by defining the following auxiliary variables:

- $z_i(k) = \delta_{f,i}^{stop}(k)\nu_{f,i}(k)$ for $i = 1, \ldots, n_f$,
- $z_j(k) = \delta_{b,j}^{stop}(k)\nu_{b,j}(k)$ for $j = 1, \ldots, n_b$,
- $[\delta_{HP}(k) = 1] \leftrightarrow [H_D(k) \geqslant H_{SFC}(k)]$, and $z_{HP}(k) = \delta_{HP}(k)u_{SFC}(k)$

The inequality constraints corresponding to the above auxiliary variables and logical statements can be obtained according to (22). In this way, the system dynamics and the constraints are formulated as mixed-integer linear equations.

5.2. Model predictive control

To provide the optimal scheduling, we apply model predictive control (MPC) [32,33]. MPC is an online control technique that relies on a dynamic model of the process, is aimed at optimising a criterion and is capable of handling constraints on inputs or outputs in a systematic way. In MPC, at each iteration the optimal control sequence is computed over a finite horizon, i.e. a finite period of time. MPC uses the receding horizon principle, which means that, after computation of the optimal control sequence, only the first sample is implemented in the next iteration. Subsequently, the horizon is shifted forward one sample and the optimisation restarts with new information on the measurements.

As mentioned before, the objective is to minimise the cost of energy production and degradation of the battery and fuel cell. Hence, the objective function for the optimisation problem can be defined as $J(k) = \alpha_1 J_{\mathrm{prod}}(k) + \alpha_2 J_{deg}(k)$, where α_1 and α_2 are weighting factors. The production cost is defined as

$$\begin{aligned} J_{\mathrm{prod}}(k) &= \Delta t\cdot \mathrm{Pr}_{e,grid}\cdot P_{e,grid}(k) \\ &+ \left(\frac{\Delta t}{\eta_e\cdot HHV_{H_2}}\mathrm{Pr}_{H_2} + C_{SFC}\right)u_{SFC}(k) \\ &+ \sum_{i=1}^{n_f}\left(\frac{\Delta t}{\eta_e\cdot HHV_{H_2}}\mathrm{Pr}_{H_2} + C_f\right)u_{f,i}(k) \\ &+ \sum_{j=1}^{n_b}(\Delta t\mathrm{Pr}_{e,grid} + C_b)u_{b,i}(k)\cdot\frac{1}{\eta_{dis}\cdot\eta_{ch}}, \end{aligned} \tag{23}$$

where $\mathrm{Pr}_{e,grid}$ is the price of electricity bought from the grid, $HHV_{H_2} = 39.41$ [kWh/kg] is the higher heating value of hydrogen, Pr_{H_2} is the price of hydrogen bought from the grid, C_{pu} is the operation and maintenance cost of each production unit (stationary fuel cell, FCEV, or BEV), and η_{ch} is the charging efficiency of BEVs.

The cost function for degradation of battery and fuel cell is defined as

$$\begin{aligned} J_{\mathrm{deg}}(k) = &\omega_{SFC}|\nu_{SCF}(k) - \nu_{SFC}(k-1)| \\ &+\omega_f\sum_{i=1}^{n_f}|\nu_{f,i}(k) - \nu_{f,i}(k-1)| \\ &+\omega_b\sum_{j=1}^{n_b}|\nu_{b,j}(k) - \nu_{b,j}(k-1)|, \end{aligned} \tag{24}$$

where ω_{pu} is the degradation cost of each production unit (stationary fuel cell, FCEV, or BEV).

Having defined the objective function and the constraints, the MPC optimisation problem with prediction horizon N_p at each time step k is defined as

$$\min_{\tilde{u}(k)} \sum_{j=0}^{N_p-1} J(k+j) \tag{25}$$

$$\text{subjectto } C(k)\nu(k-1) + D(k)\tilde{u}(k) \leqslant g(k) \tag{26}$$

where $J(k)$ is the weighted sum of (23) and (24), $\tilde{u}(k) = [u^T(k), u^T(k+1), \ldots, u^T(k+N_p-1)]^T$ is the stacked vector of control variables (both continuous and binary), $C(k)$, $D(k)$ and $g(k)$ are constraint matrices and the constant vector, respectively, defined based on constraint Eqs. (14)–(20) and the MLD constraints obtained from (22). The optimisation problem (25) and (26) is a mixed-integer linear programming (MILP) problem, which can be solved using the available MILP solvers [34,35].

5.3. Results of optimal scheduling

The optimisation problems were solved using the MILP solver from Gurobi in Matlab R2018b on a 3.1 GHz Intel Core i5 processor. We produced the optimal schedule for 48 h based on the building's load profile data from two days in February 2017. The time step Δt is one hour and for every time step we assumed that all the EVs were available, using the building's entire parking capacity, which is 454 cars.

Remark. *The optimisation model can be adjusted to limit the number of cars available at every time step or to take into account more details about their driving patterns.*

We assumed the following power capacity limits for each production unit: $0 \leqslant u_{SFC} \leqslant 1400$, $3 \leqslant u_{f,i} \leqslant 20$, $3.5 \leqslant u_{b,j} \leqslant 10.4$ for $i = 1, \ldots, n_f$ and $j = 1, \ldots, n_b$. Moreover, we assumed that the battery of a BEV has a capacity of 60 kWh and that the state of charge of each car at the beginning of each day (00:00 h) was 80%, i.e. 48 kWh. Also, BEVs were not allowed to remain in V2G mode once their state of charge had fallen to 20%. The tank-to-wheel efficiency of the fuel cell for electricity production was 60% in our model, and for heat production it was 24%. We also assumed that the discharge efficiency of a BEV battery is 80.8% and its charging efficiency is 90.7% [36,37]. The weighting factors in the objective function were set at $\alpha_1 = \alpha_2 = 1$ and the degradation costs at $\omega_f = \omega_b = 0.1$€and $\omega_{SFC} = 0.05$€. The price of electricity bought from the grid was set at 0.042 €/kWh and that of hydrogen at 2.54 €/kg. These choices were based on the cost calculations in the previous sections, and also to ensure that the controller would use both types of EVs. We have observed that if the price of hydrogen and electricity are very close, the controller will not use BEVs as they result in higher production costs. For illustration purposes, we therefore did not use the exact values obtained for electricity and hydrogen in Section 4.2, Table 4 and Section 4.1, Table 2.

Fig. 16 shows the optimisation results for a 48-h period. In it we see the demand for power and the power generated by each of the production sources. The solid-cross line shows local solar power generation at the building. The solid line shows power demand after subtracting local solar power generation and the dashed line shows total power generation; since this supply matches the building's demand, these two

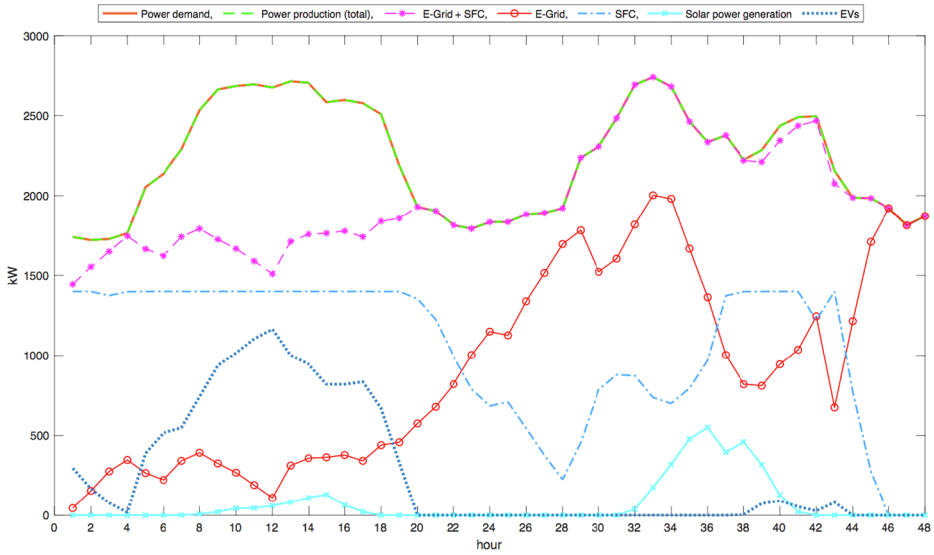

Fig. 16. Power demand and power production profile at the office during 48 h.

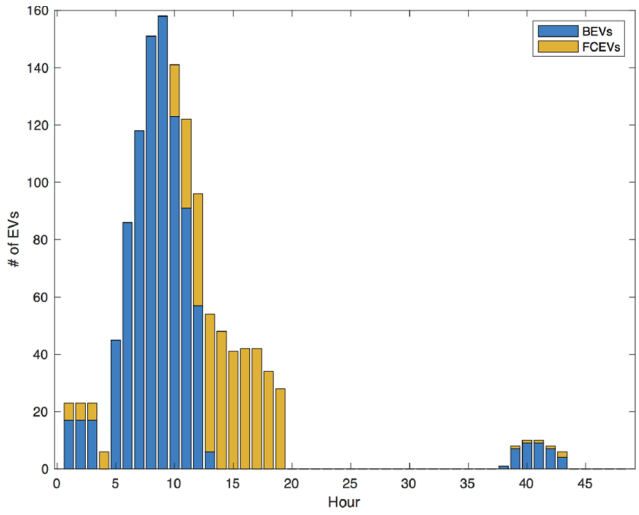

Fig. 17. Number of EVs used for balancing the supply and demand at the office during 48 h.

lines are coincident in the figure. The solid-circle line shows the amount of power bought from the electricity grid, based on the wind profile and grid availability. The wind profile over these two days is a good indicator of one relatively calm day (the first) and one windier one (the second). As mentioned before, since the production capacity of the solar panels is much lower than the building's demand, due to its lab activities, solar is never enough by itself to satisfy that demand. As shown in this figure, on the first day and most of the second, wind production is also way below the building's demand (even after including solar power generation) and so other energy sources are needed.

Based on the system objectives of minimising both energy costs and the degradation of batteries and fuel cells (cf. Eqs. (23)), the controller first buys power from the grid (solid-circle line), then uses the stationary fuel cell (dash-dot line). As can be seen on the first day with less wind, even though the stationary fuel cell is used at maximum capacity for most of the day, the sum of the power it generates and that bought from the grid (dash-star line) does not satisfy total demand. This is also the case for few hours on the second day. These periods are when we either have peak load or a supply-demand mismatch due to limited production capacity and the intermittent renewable sources. At these times, both BEVs and FCEVs are used for balancing purposes (dotted line), i.e. match supply with demand.

Based on this control strategy, the total cost of the energy production on these two days is 9045 €. Without optimal scheduling and considering only the system constraints in the production planning, the total generation cost would have been 9308 €. Although the saving derived from optimal scheduling does not seem significant over two days, it would be if it were applied for the entire year.

Fig. 17 shows the number of cars used during the peak hours and the hours of mismatch between supply and demand.

As can be seen here, based on the electricity price and the hydrogen price obtained in our model, the controller first mostly uses BEVs and then FCEVs. Note that since we only use BEVs down to 20% of their state of charge, after a few hours they are no longer available. FCEVs, however, since we assume that in V2G mode they are connected directly to the hydrogen grid and we do not use the tank, are always available unless and until our fair-use constraints (cf. (18) and (19)) preclude further utilisation. In this optimisation model, we assume that each EV can be used for four hours at a time, i.e., $T = 4$ in (18), and that once used in V2G mode it becomes unavailable for the next 12 h, i.e. $T' = 12$ in (19). These values have been chosen considering the actual availability of vehicles at the location. The advantage of optimal scheduling is thus its more systematic and fair usage of the EVs (compare Fig. 17 with Fig. 15) and hence its ability to provide greater incentives for car owners to participate in the V2G plan.

Note that we include only energy production costs in our optimisation model, not investment costs. That is why BEVs are used more than FCEVs at the times when they are both available. In practice, however, given the investment costs for the V2G infrastructure and for bidirectional chargers for FCEVs and BEVs, respectively (cf. Table A.9), there are likely to be more V2G points for FCEVs than for BEVs. And this will change the choices made by the controller. Another important observation regarding this model is that even during peak hours we need fewer than 160 cars. That represents less than half of this building's parking capacity. Our results thus indicate that including cars for balancing and back-up power in the energy system of an office block, and of other buildings in general, is a viable solution and adds both flexibility and reliability to its power supply.

6. Conclusions and discussions

In this paper we have presented the concept design and energy management of a 100% renewable energy system for a real-life environment: the Shell Technology Centre in Amsterdam. The result is an integrated energy and mobility system in which we use both electricity

and hydrogen as energy carriers and both battery and hydrogen-based fuel cell electric vehicles to deliver electricity to the office grid at times when they are parked there. In this design, we investigate the feasibility of such an integrated system at a real-life environment. We have considered two different time periods – Near Future (2025–2030) and Mid-Century (2040–2050) – and three different scenarios: 1) Hydrogen-Electric; 2) All-Electric; and 3) Combined.

For each of these periods and scenarios, we have conducted a techno-economic analysis to compare the system levelized cost of energy for the building's entire energy system. Furthermore, in order to make systematic and fair use of EVs in V2G mode and to improve the operational performance of the energy system, we have devised an optimal scheduling using model predictive control. Our objective was to minimise degradation of the cars' batteries and fuel cells as well as to minimise the system's energy production costs.

From the results obtained in respect of the three scenarios we investigated, we conclude that the Combined one results in the lowest system levelized cost of energy at the STCA. Furthermore, as in the current energy system, we have observed that, in one system based on 100% renewable sources, between 20 and 30% of the energy supplied comes from storage. This emphasises the important role of storage and its cost in such a system design. As we have seen in our study, storage using hydrogen and salt caverns is much cheaper than using electricity and large batteries. Based on our simulation results, we also conclude that not that many cars are needed for load balancing during peak hours and at times of mismatch between supply and demand. The economic figures show that creating such a system at an office building is both economically and technically feasible, and that including electric vehicles in it provides a flexible energy buffer. Moreover, the results of the optimal scheduling shows that it can improve the efficiency and decrease cost of production even further. Ultimately, the results of this study bring us to conclusion that using both electricity and hydrogen as energy carriers leads to a more flexible, more reliable and cheaper energy system at an office building.

The next step is to provide the necessary infrastructure and incentives for the implementation of such an integrated energy and mobility system, especially for buildings with large parking areas such as office blocks, hospitals and airports. In this paper we have taken the first step towards shaping a fair use of electric vehicles in vehicle-to-grid mode. Further investigation in this area is required in order to provide effective economic incentives for vehicle owners. One option is to give them a discount on the cost of their fuel based on the kWh they deliver to the electricity grid. Another is that building owners or energy companies own the vehicles and lease them to public users. Furthermore, the infrastructure for vehicle-to-grid solutions and hydrogen refuelling stations needs to be in place in order to be able to implement such integrated systems. Other options, such as heat storage in tanks or underground aquifers, could be also included in the design as alternatives or to complement heat pumps and boilers.

CRediT authorship contribution statement

Samira S. Farahani: Writing - original draft, Conceptualization, Methodology, Formal analysis, Supervision, Project administration. **Cliff Bleeker:** Formal analysis, Investigation, Methodology. **Ad van Wijk:** Supervision, Funding acquisition, Conceptualization, Validation, Writing - review & editing. **Zofia Lukszo:** Supervision, Funding acquisition, Project administration, Validation, Writing - review & editing.

Declaration of Competing Interest

The authors declare that they have no known competing financial interests or personal relationships that could have appeared to influence the work reported in this paper.

Acknowledgments

This research is supported by Shell Technology Center in Amsterdam and we are thankful to their staff who helped us with the data collection and analysis during this project.

Appendix A. Component parameters

In Table A.9 the investment cost, operation and maintenance cost, and life time of each unit used in the energy system of the Shell office is presented. In Table A.10 the fixed cost of storage, infrastructure and external EV charging and refueling are presented.

Table A.9
Component Parameters for model analysis; all efficiencies are calculated using HHV (η: efficiency; cf: capacity factor; IC: installed investment cost; O&M: operation and maintenance; LT: economic lifetime).

Components	Near Future				Mid-Century			
	η or cf [%, –]	IC [€/kW]	O&M [%/y]	LT [y or h]	η or cf [%, –]	IC [€/kW]	O&M [%/y]	LT [y or h]
Electricity production								
PV System [38–41]	0.10 cf	725	2.8	25	0.12	440	2.3	30
Wind turbine [42–44]	0.59	1728	3.7	20	0.59	1390	3.7	30
Hydrogen production and transport								
Electrolyzer [45–48]	77%	480	2	20	82%	200	2	30
Compressor [49,50]	1.5 kWh/kg H_2	8060	4	15	1 kWh/kg H_2	3440	2	15
Hydrogen consumption								
Stationary fuel cells [51–53]	60%η_e/20%η_q	512	2.5	60000 h	65%η_e/15%η_q	200	2.5	90000 h
Heating and Cooling Components								
Hydrogen boilers (kW heat) [54]	97%	100	1.3	35	97%	100	1.3	35
Air-conditioning system (kW heat) [55]	4.13 COP	240	4.3	20	4.43 COP	240	4.3	20
Heat pump (kW heat) [54,56]	4.1 COP_{avg}	700	0.7	20	4.2 COP_{avg}	490	0.7	20
Electric components								
Lithium-ion Batteries (BEVs) for V2G only [57–60]	73% total	96	1	8	95% total	70	1	15
Stationary Batteries Systems (BESS) [57–59,61,62]	87% total	300	1	10	95% total	210	1	15
Vehicle-to-grid components								
FCEV stack Replacement Costs [63,19,51]	60%η_e	40	1	4100 h	65%η_e	26.5	1	8000 h
FCEV discharge infrastructure [39]	–	6400	5	15	–	3200	5	15
BEV chargers (bi-direct) 2-point [64,65]	–	9500	5	15	–	5000	5	15

Table A.10
Fixed cost parameters for energy services used in the model.

Component	Unit	Near Future [€]	Mid-Century [€]
Salt Cavern Storage	kg^{-1} H_2	1.79	1.57
External Grid Battery	$kW\ h^{-1}$	0.155	0.09
H_2 grid infrastructure	160 kg/h	19.8 k (HE)	19.8 k (HE)
E-grid infrastructure	10 MW	216 k (AE)	216 k (AE)
External charged BEVs [65]	kWh^{-1}	0.25	0.15
Externally fueled FCEVs [65]	kg^{-1} H_2	6	4

Appendix B. Cost of components in Scenario 1

The total cost of each component used in Hydrogen-Electric scenario together with their size, capital cost, and operation and maintenance cost are presented in Table B.11.

Table B.11
Cost tables of Hydrogen-Electric System Design for near-future and mid-century scenarios (Q: installed component capacity; CC: annual capital cost; OMC: annual operation and maintenance cost; TC: total annual capital and operation and maintenance costs)

			Near Future				Mid-Century		
Type	Unit [–]	Q	CC [k€/y]	OMC [k€/y]	TC [k€/y]	Q	CC [k€/y]	OMC [k€/y]	TC [k€/y]
Solar	kW	1176	49	23.9	72.8	1176	26.4	11.9	38.3
Wind	kW	7868	914	503.1	1417.0	6225	441.5	320.2	761.6
Electrolyser	kW	8800	283.9	84.5	368.4	6600	67.3	13.2	80.5
Compressor, water treatment	kg H_2/hr	149	102.4	49.3	151.8	124	37.1	9.6	46.7
Salt Cavern	tonnes H2 Capacity	3733	0	450.9	450.9	3733	0	320	320
H-Grid	Nm^3/h Gas Grid Type	400	0	16.2	16.2	400	0	14.7	14.7
E-Grid	MW Connection Capacity	0	0	0	0	0	0	0	0
Stationary Fuel Cell	kW	1650	138.3	21.1	159.4	1596	36.6	8	44.5
FCEV	kW of systems	15600	293.2	6.2	299.4	12700	66.9	3.4	70.2
BEV	kWh of batteries	2040	6.7	2	8.6	3400	7.1	2.4	9.5
Bi-Directional Chargers	# of 2-point chargers	17	13.5	8.1	21.6	17	7.1	4.3	11.4
FCEV Discharge Infrastructure	# of 4-point connectors	39	20.9	12.5	33.4	32	8.6	5.1	13.7
Airco	kW	1900	30.6	13.7	43.3	1900	30.7	13.7	44.3
H2 Boilers	kW	1286	6	1.7	7.7	1285	6	1.7	7.7
External Charging costs BEVs	kWh	51761	0	12.9	12.9	4226.3	0	0.6	0.6
Total Costs			**1858.5**	**1206.1**	**3064.5**		**735.2**	**728.6**	**1463.8**

Appendix C. Cost of components in Scenario 2

The total cost of each component used in All-Electric scenario together with their size, capital cost, and operation and maintenance cost are presented in Table C.12 using external battery storage and in Table C.13 using a large local battery storage.

Table C.12
Cost tables of All-Electric System Design with external main storage for near-future and mid-century scenarios (Q: installed component capacity; CC: annual capital cost; OMC: annual operation and maintenance cost; TC: total annual capital and operation and maintenance costs).

			Near Future				Mid-Century		
Type	Unit [–]	Q	CC [k€/y]	OMC [k€/y]	TC [k€/y]	Q	CC [k€/y]	OMC [k€/y]	TC [k€/y]
Solar	kW	1176	49	23.9	72.8	1176	26.4	11.9	38.3
Wind	kW	3990	463.5	255.1	718.6	3027	214.7	155.7	370.3
Electrolyser	kW	200	6.5	1.9	8.4	200	2	0.4	2.4
Compression, water treatment	kg/h	2.9315	2	1	3	2.6656	0.8	0.2	1
Salt Cavern	kg H2 Capacity	3733	0	12.4	12.4	1000	0	9.9	9.9
H-Grid	Nm^3/h NG grid type	40	0	2.4	2.4	40	0	2.4	2.4
E-Grid	MW Connection Capacity	10	0	216.2	216.2	10	0	216.2	216.2
Stationary Battery (BESS)	kWh	12000	422	36	458	9000	158.3	18.9	177.2
FCEV	kW of systems	15400	123.7	6.2	129.9	12600	27.4	3.3	30.7
BEV	kWh of batteries	17820	155	17.1	172.1	28500	123.2	20	143.2
Bi-Directional Chargers	2-point chargers	149	118.6	70.8	189.3	143	59.9	35.8	95.6
FCEV Discharge Infrastructure	4-point connectors	39	20.9	12.5	33.4	32	17.2	10.2	27.4
Heat Pump	kW	3300	155.3	16.2	171.4	2970	139.7	14.6	154.3
External Grid Storage	MWh	2190	0	229.1	229.1	1243	0	67.1	67.1
External Fuelling Costs FCEV	tons	49	0	292.1	292.1	27	0	108.1	108.1
External Charging Costs BEVs	MWh	1973	0	493.3	493.3	3035	0	455.4	455.4
Total Costs			**1516.5**	**1686.1**	**3202.6**		**769.6**	**1129.9**	**1899.5**

Table C.13
Cost tables of All-Electric System Design with big battery for near-future and mid-century scenarios (Q: installed component capacity; CC: annual capital cost; OMC: annual operation and maintenance cost; TC: total annual capital and operation and maintenance costs).

Type	Unit	Near Future				Mid-Century		
	[–]	Q	CC [k€]	OMC [k€]	TC [k€]	Q	CC [k€]	OMC [k€]	TC [k€]
Solar	kW	1176	49	23.9	72.8	1176	26.4	11.9	38.3
Wind	kW	3990	463.5	255.1	718.6	3027	214.7	155.7	370.3
Electrolyser	kW	200	6.5	1.9	8.4	200	2	0.4	2.4
Compression, water treatment	kg/h	2.9315	2	1	3	2.6656	0.8	0.2	1
Salt Cavern	tons H2 Capacity	3733	0	12.4	12.4	1000	0	9.9	9.9
H-Grid	Nm^3/h NG equivalent	40	0	2.4	2.4	40	0	2.4	2.4
E-Grid	MW Connection Capacity	10	0	216.2	216.2	10	0	216.2	216.2
Stationary Battery (BESS)	kWh	200000	9378.4	480	9858.4	200000	5026	360	5386
FCEV	kW of systems	15400	123.7	6.2	129.9	12600	27.4	3.3	30.7
BEV	kWh of batteries	17820	155	17.1	172.1	28500	123.2	20	143.2
Bi-Directional Chargers	2-point chargers	149	118.6	70.8	189.3	143	59.9	35.8	95.6
FCEV Discharge Infrastructure	4-point connectors	39	20.9	12.5	33.4	32	17.2	10.2	27.4
Heat Pump	kW	3300	155.3	16.2	171.4	2970	139.7	14.6	154.3
Electricity Market (bought)	MWh	1374	0	252	252	829	0	165.9	165.9
Electricity Market (Sold)	MWh	909	0	0	0	598	0	0	0
External Fuelling Costs FCEV	tons	28	0	167.9	167.9	16	0	95.6	95.6
External Charging CostS BEV	MWh	2495	0	104.6	104.6	3629	0	142.4	142.4
Total Costs			**10472.9**	**1640.2**	**12113.1**		**5637.3**	**1244.5**	**6881.8**

Appendix D. Cost of components in Scenario 3

The total cost of each component used in combined scenario together with their size, capital cost, and operation and maintenance cost are presented in Tables D.14, D.15 and D.16 for each of the Cases 1–3, respectively.

Table D.14
Cost tables of Combined System Design for near-future and mid-century scenarios with use of heat pump (Q: installed component capacity; CC: annual capital cost; OMC: annual operation and maintenance cost; TC: total annual capital and operation and maintenance costs).

Type	Unit [–]	Near Future				Mid-Century			
		Q	CC [k€/y]	OMC [k€/y]	TC [k€/y]	Q	CC [k€/y]	OMC [k€/y]	TC [k€/y]
Solar	kW	1176	49	23.9	72.8	1176	26.4	11.9	38.3
Wind	kW	5800	673.7	370.8	1044.5	4800	340.4	246.9	587.3
Electrolyser	kW	6600	212.9	63.4	276.3	4400	44.9	8.8	53.7
Compression, water treatment	kg/h	94	64.3	30.9	95.2	84.638	24.9	6.2	31.1
Salt Cavern	tonnes H2 Capacity	3733	0	343.3	343.3	3733000	0	258.2	258.2
H-Grid	Nm^3/h NG	400	0	15	15	400	0	13.6	13.6
E-Grid	MW Connection Capacity	10	0	216.2	216.2	10	0	216.2	216.2
Stationary Fuel Cell	kW	1450	121.5	18.6	140.1	1400	32.1	7	39.1
FCEV	kW of systems	17800	93.7	7.1	100.8	15700	27.7	4.2	31.9
BEV	kWh of batteries	4440	13.6	4.3	17.8	5600	11.8	3.9	15.7
Bi-Directional Chargers	# of 2-point chargers	37	29.4	17.6	47	28	11.7	7	18.7
FCEV Discharge Infrastructure	# of 4-point connectors	45	24.1	14.4	38.5	40	10.7	6.4	17.1
Heat Pumps	kW	3300	108.7	11.3	120	2970	97.8	10.2	108
External Charging costs BEVs	MWh	84	0	20.9	20.9	32.3643	0	4.9	4.9
Total Costs			**1391**	**836.6**	**2227.6**		**628.4**	**648.9**	**1277.3**

Table D.15
Cost tables of Combined System Design for near-future and mid-century scenarios with use of boilers and SFC (Q: installed component capacity; CC: annual capital cost; OMC: annual operation and maintenance cost; TC: total annual capital and operation and maintenance costs).

		Near Future				Mid-Century		
Type	Unit [–]	Q	CC [k€/y]	OMC [k€/y]	TC [k€/y]	Q	CC [k€/y]	OMC [k€/y]	TC [k€/y]
Solar	kW	1176	49	23.9	72.8	1176	26.4	11.9	38.3
Wind	kW	6000	696.9	383.6	1080.5	5100	361.7	262.3	624
Electrolyser	kW	6600	212.9	63.4	276.3	6600	67.3	13.2	80.5
Water Purification	m3/day	9	0.6	0.5	1.1	8.016	0.6	0.5	1
Pure Water Tank	m3	18	0.1	0	0.1	16.032	0.1	0	0.1
Salt Cavern	tonnes H2 Capacity	3733	0	307.1	307.1	3733	0	249.9	249.9
H-Grid	Nm^3/h NG Equivalent	400	0	15.2	15.2	400	0	14	14
E-Grid	MW Connection Capacity	10	0	216.2	216.2	10	0	216.2	216.2
Stationary Fuel Cell	kW	1400	117.3	17.9	135.2	1250	28.6	6.3	34.9
FCEV	kW of systems	17800	85.9	7.1	93	16100	29.3	4.3	33.6
BEV	kWh of batteries	3660	11.3	3.5	14.8	5000	10.5	3.5	14
Bi-Directional Chargers	# of 2-point chargers	31	24.7	14.7	39.4	25	10.5	6.3	16.7
FCEV Discharge Infrastructure	# of 4-point connectors	45	24.1	14.4	38.5	41	11	6.6	17.6
H2 boilers	kW	1748	8.1	2.3	10.4	1573.4068	7.3	2	9.4
Airco	kW	1900	30.7	13.7	44.3	1900	30.7	13.7	44.3
External Charging costs BEVs	MWh	71	0	17.9	17.9	37	0	5.6	5.6
Total Costs		**0**	**1261.6**	**1101.3**	**2362.9**	0	**583.9**	**816.2**	**1400.1**

Table D.16
Cost tables of Combined System Design for near-future and mid-century scenarios with fixed electricity and hydrogen grid costs (Q: installed component capacity; CC: annual capital cost; OMC: annual operation and maintenance cost; TC: total annual capital and operation and maintenance costs).

		Near Future				Mid-Century		
Type	Unit [–]	Q	CC [k€/y]	OMC [k€/y]	TC [k€/y]	Q	CC [k€/y]	OMC [k€/y]	TC [k€/y]
Solar	kW	1176	49	23.9	72.8	1176	26.4	11.9	38.3
Stationary Fuel Cell	kW	1400	117.3	17.9	135.2	1250	28.6	6.3	34.9
FCEV	kW of systems	15400	95.8	6.2	102	13700	29.6	3.6	33.3
BEV	kWh of batteries	3960	12.5	3.8	16.3	6000	12.6	4.2	16.8
Bi-Directional Chargers	# of 2-point chargers	33	26.3	15.7	41.9	30	12.6	7.5	20.1
FCEV Discharge Infrastructure	# of 4-point connectors	39	20.9	12.5	33.4	35	9.4	5.6	15
Heat Pumps	kW	3300	108.7	11.3	120	2970	97.8	10.2	108
External Charging costs BEVs	MWh	86	0	21.5	21.5	429	0	6.4	6.4
Bought H2 from grid	tonnes	584	0	1821.2	1821.2	483	0	918.4	918.4
Bought E from grid	MWh	426	0	289.9	289.9	3656	0	171.9	171.9
Total Costs			**430.4**	**2223.8**	**2654.3**		**217.1**	**1146**	**1363.1**

Appendix E. Yearly energy distribution in Case 1 of Combined scenario

Figs. E.18 and E.19 show the Sankey diagrams for the annual energy balance at the office in Case 1 of Combined scenario in near future and mid-century, respectively, and the energy flows to and from each component in the energy. system.

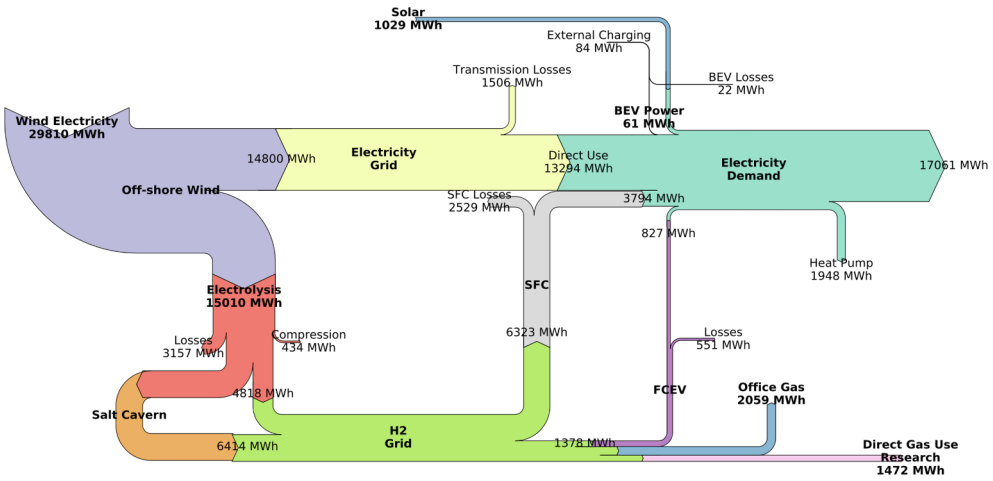

Fig. E.18. Sankey diagram showing the annual energy balance for a fully renewable electricity, heating, and transport system at the office in near future for Case 1 of Combined scenario.

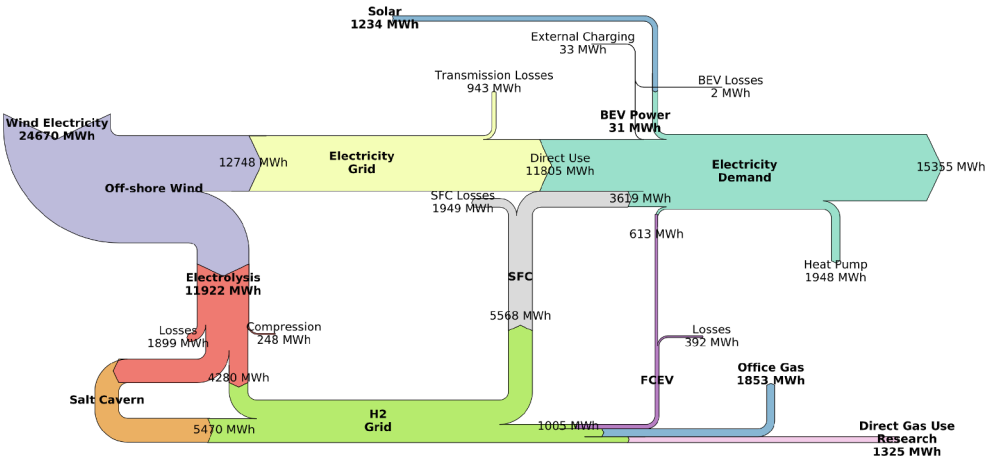

Fig. E.19. Sankey diagram showing the annual energy balance for a fully renewable electricity, heating, and transport system at the office in mid-century for Case 1 of Combined scenario.

Appendix F. Cost distribution of investment costs and operational & maintenance costs

Figs. F.20–F.22 illustrate the cost distribution of investment costs and operational & maintenance costs for each of the three scenarios.

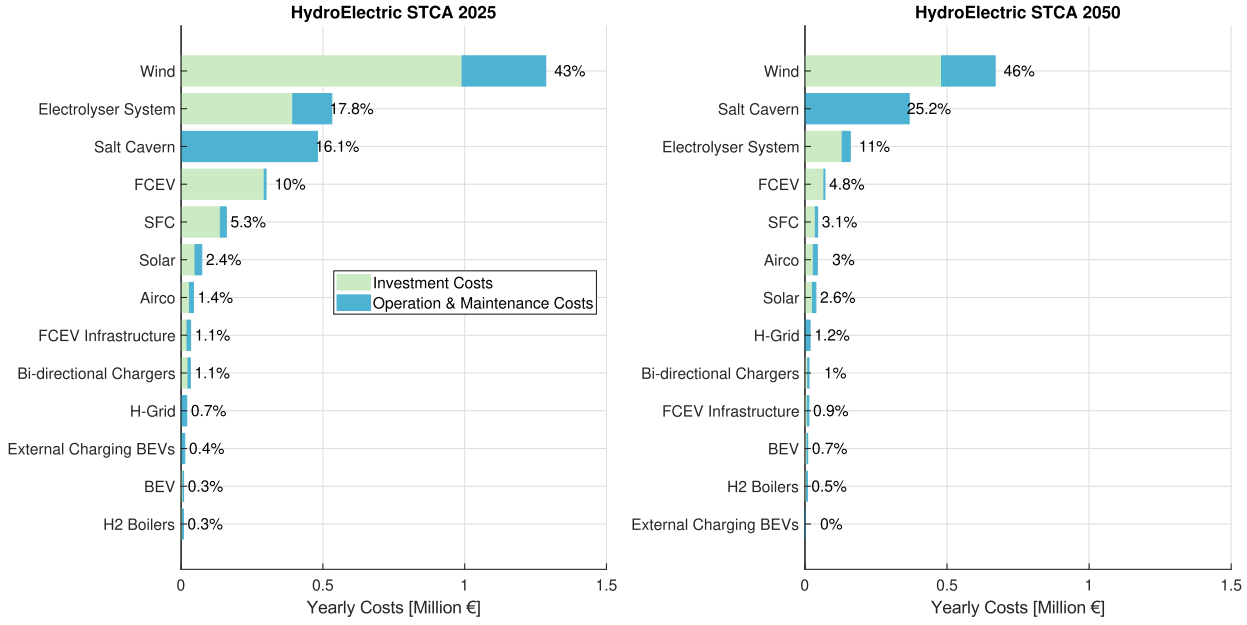

Fig. F.20. Cost distribution of Investment Costs and Operational & Maintenance costs for the Hydrogen-Electric scenario. Percentages in chart are shown compared to Total System Cost (TSC) presented in Table B.11.

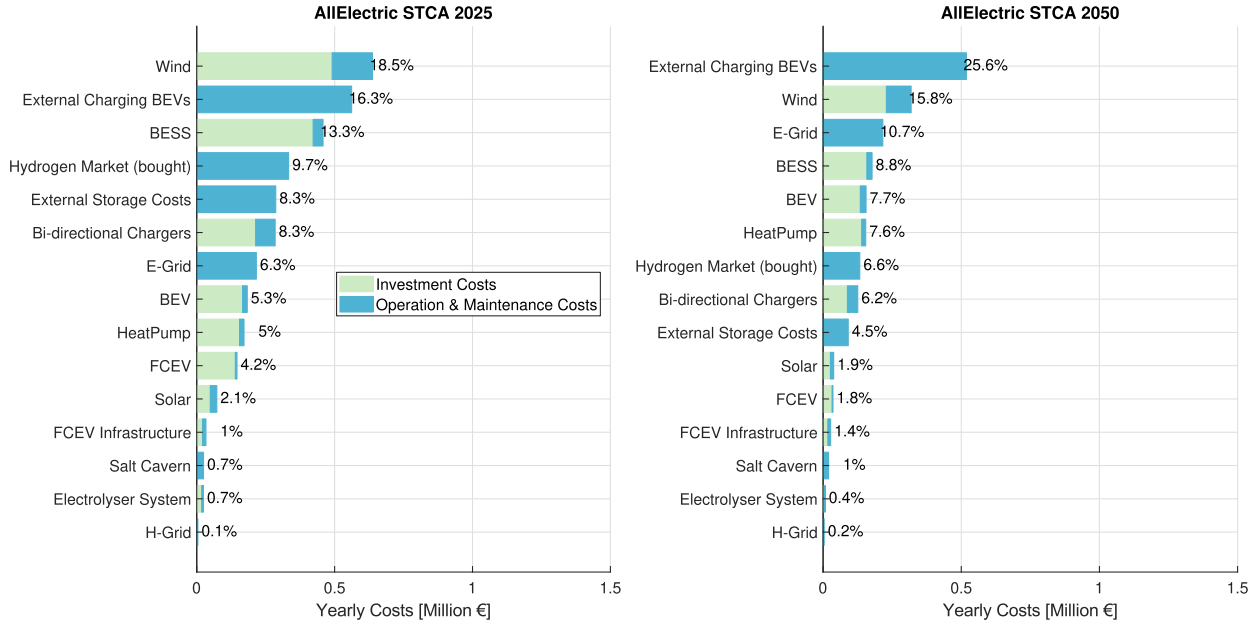

Fig. F.21. Cost distribution of Investment Costs and Operational & Maintenance costs for the All-Electric scenario. Percentages in chart are shown compared to Total System Cost (TSC) presented in Table C.12 using an external battery storage.

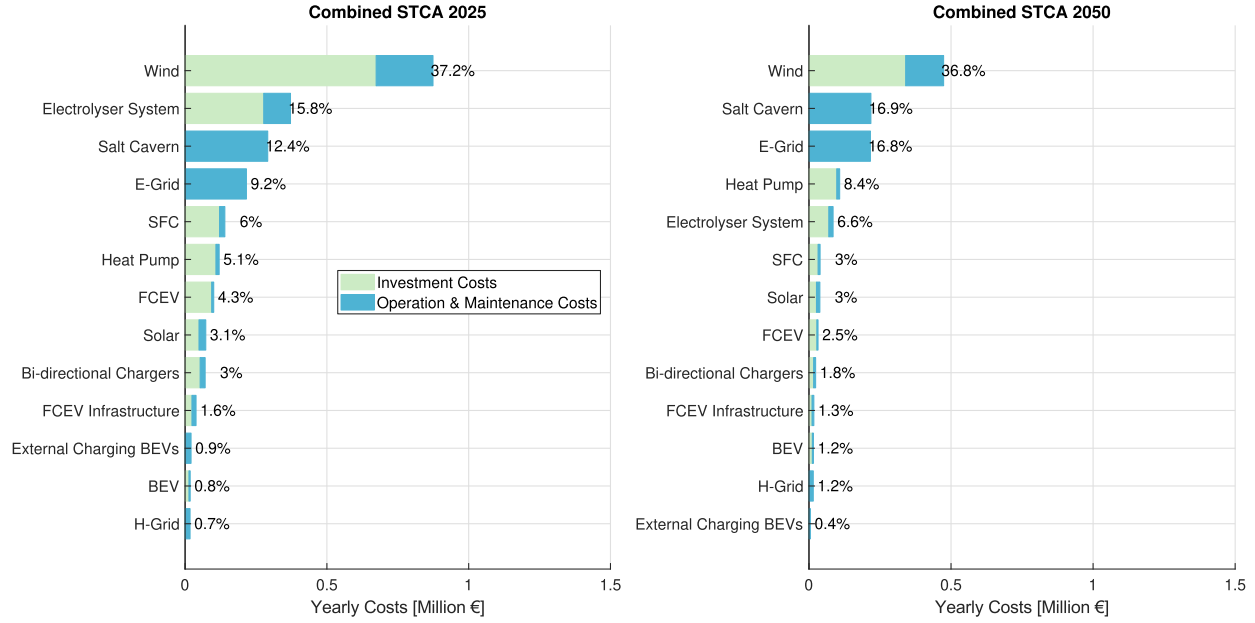

Fig. F.22. Cost distribution of Investment Costs and Operational & Maintenance costs for the Combined scenario Case 1 (using heat pumps). Percentages in chart are shown compared to Total System Cost (TSC) presented in Table D.14.

References

[1] United Nations (UN). Adoption of the Paris agreement eframework convention on climate change, 2015. https://unfccc.int/resource/docs/2015/cop21/eng/l09r01.pdf.

[2] van Wijk A, Verhoef L. Our car as power plant. Amsterdam, Netherlands: IOS Press BV; 2014.

[3] Habib S, Kamran M, Rashid U. Impact analysis of vehicle-to-grid technology and charging strategies of electric vehicles on distribution networks a review. J Power Sources 2015;277:205–14.

[4] Kempton W, Tomic J, Letendre S, Brooks A, Lipman T. Vehicle-to-grid power: battery, hybrid, and fuel cell vehicles as resources for distributed electric power in california. Technical report, Institute of Transportation Studies; 2001.

[5] Farahani SS, van der Veen R, Oldenbroek V, Park Lee E, van de Wouw N, van Wijk AJM, De Schutter B, Lukszo Z. Hydrogen-based integrated energy and transport system. IEEE Syst Man Cybernet Mag 2019;5(1):27–50.

[6] Brown T, Schlachtberger D, Kies A, Schramm S, Greiner M. Synergies of sector coupling and transmission reinforcement in a cost-optimised, highly renewable european energy system. Energy 2018;160:720–39.

[7] Cao S. Comparison of the energy and environmental impact by integrating a H2 vehicle and an electric vehicle into a zero-energy building. Energy Convers Manage 2016;123:153–73.

[8] Garmsiri S, Koohi-Fayegh S, Rosen MA, Smith GR. Integration of transportation energy processes with a net zero energy community using captured waste hydrogen from electrochemical plants. Int J Hydrogen Energy 2016;41:8337–46.

[9] Mathiesen BV, Lund H, Connolly D, Wenzel H, Østergaard PA, Möller B, Nielsen S, Ridjan I, Karnøe P, Sperling K, Hvelplund FK. Smart energy systems for coherent 100% renewable energy and transport solutions. Appl Energy 2015;145:139–54.

[10] Steward D, Zuboy J. Community energy: analysis of hydrogen distributed energy systems with photovoltaics for load leveling and vehicle refueling. National Renewable Energy Laboratory; 2014.

[11] Andrews J, Shabani B. Re-envisioning the role of hydrogen in a sustainable energy economy. Int J Hydrogen Energy 2012;37:1184–203.

[12] Evangelopoulou S, De Vita A, Zazias G, Capros P. Energy system modelling of carbon-neutral hydrogen as an enabler of sectoral integration within a decarbonization pathway. Energies 2019;12(13):2551–74.
[13] Teichmann D, Arlt W, Wasserscheid P. Liquid organic hydrogen carriers as an efficient vector for the transport and storage of renewable energy. Int J Hydrogen Energy 2012;37(23):18118–32.
[14] Michalski J, Bnger U, Crotogino F, Donadei S, Schneider GS, Pregger T, Cao K, Heide D, et al. Hydrogen generation by electrolysis and storage in salt caverns: potentials, economics and systems aspects with regard to the german energy transition. Int J Hydrogen Energy 2017;42(19):13427–43.
[15] Ozarslan A. Large-scale hydrogen energy storage in salt caverns. Int J Hydrogen Energy 2012;37(19):14265–77.
[16] Niemi R, Mikkola J, Lund PD. Urban energy systems with smart multi-carrier energy networks and renewable energy generation. Renewable Energy 2012;48:524–36.
[17] Shao C, Wang X, Shahidehpour M, Wang X, Wang B. An milp-based optimal power flow in multicarrier energy systems. IEEE Trans Sustain Energy 2017;8(1):239–48.
[18] Oldenbroek V, Hamoen V, Alva S, Robledo C, Verhoef L, van Wijk AJM. Fuel cell electric vehicle-to-grid: experimental feasibility and operational performance. In: Proceedings of the 6th European PEFC & electrolyser forum, Lucerne, Switzerland, June 2017.
[19] Oldenbroek V, Verhoef LA, van Wijk AJM. Fuel cell electric vehicle as a power plant: fully renewable integrated transport and energy system design and analysis for smart city areas. Int J Hydrogen Energy 2017;42:8166–96.
[20] Alavi F, Park Lee EH, van de Wouw N, De Schutter B, Lukszo Z. Fuel cell cars in a microgrid for synergies between hydrogen and electricity networks. Appl Energy 2017;192:296–304.
[21] Alavi F, van de Wouw N, De Schutter B. Power scheduling in islanded-mode microgrids using fuel cell vehicles. In: Proceedings of the 56th IEEE Conference on Decision and Control (CDC), Melbourne, Australia, December 2017.
[22] Park Lee EH, Chappin E, Lukszo Z, Herder P. The car as power plant: towards socio-technical systems integration. In. Proceedings of IEEE PowerTech, Eindhoven, the Netherlands, June-July. 2017.
[23] Park Lee EH, Lukszo Z, Herder P. Aggregated fuel cell vehicles in electricity markets with high wind penetration. In: Proceedings of IEEE International Conference of Networking, Sensing and Control (ICNSC), Zhuhai, China, March 2018.
[24] van der Veen R, Verzijlbergh R, Lukszo Z. Exploring the profit potential of energy storage in a car park using electrolysis, hydrogen storage and fuel cell electric vehicles. In: Proceedings of the international conference on Sustainable Energy & Environmental Protection (SEEP2017), Bled, Slovenia, June 2017.
[25] American Petroleum Institute. Energy infrastructure: underground natural gas storage; 2017. https://energyinfrastructure.org/energy-101/natural-gas-storage/.
[26] Moomaw W, Burgherr P, Heath G, Lenzen M, Nyboer J, Verbrugge A. Annex II: methodology in IPCC special report on renewable energy sources and climate change mitigation. Cambridge, UK and New York, NY: Cambridge University Press; 2011.
[27] Blok K, Nieuwlaar E. Introduction to energy analysis. 2nd ed. London, UK: Routledge; 2016.
[28] Stichting Simular. Milieubarometer kantoor; 2014. https://www.milieubarometer.nl/voorbeelden/kantoor/.
[29] CE Delft. Net voor de toekomst; 2017. https://www.netbeheernederland.nl/_upload/Files/Achtergrondrapport_Net_voor_de_toekomst_113.pdf.
[30] KIWA Technology. Toekomstige gasdistributienetten. Technical report, Netbeheer Nederland; 2018.
[31] Bemporad A, Borrelli F, Morari M. Model predictive control based on linear programming – the explicit solution. IEEE Trans Autom Control 2002;47(12):1974–85.
[32] Camacho EF, Bordons C. Model predictive control in the process industry. Berlin, Germany: Springer-Verlag; 1995.
[33] Maciejowski JM. Predictive control with constraints. Harlow, England: Prentice Hall; 2002.
[34] Atamtürk A, Savelsbergh MWP. Integer-programming software systems. Ann Oper Res 2005;140(1):67–124.
[35] Linderoth JT, Ralphs TK. Noncommercial software for mixed-integer linear programming. In: Karlof J, editor, Reinforcement learning: state-of-the-art, CRC Press Operations Research Series; 2005. p. 253–303.
[36] Apostolaki-Iosifidou E, Codani P, Kempton W. Measurement of power loss during electric vehicle charging and discharging. Energy March 2017;127:730–42.
[37] Simpson M. Spiders bi-directional charging station interconnection testing. Technical report, Renewable Energy Laboratory; 2013.
[38] Honrubia-Escribano A, Ramirez FJ, Gmez-Lzaro E, Garcia-Villaverde PM, Ruiz-Ortega MJ, Parra-Requena G. Influence of solar technology in the economic performance of pv power plants in europe. a comprehensive analysis. Renew Sustain Energy Rev 2018;82:488–501.
[39] ISE Fraunhofer and Agora Energiewende. Current and future cost of photovoltaics. long-term scenarios for market development, system prices and lcoe of utility-scale pv systems. Agora Energiewende, 82; 2015.
[40] International Renewable Energy Agency (IRENA). Renewable power generation costs in 2017. Technical report; 2018.
[41] International Renewable Energy Agency (IRENA). The power to change: Solar and wind cost reduction potential to 2025. Technical report; 2016.
[42] KIC InnoEnergy. Future renewable energy costs: Offshore wind. update 2017. Technical report; 2017.
[43] Fraunhofer Institute for Systems and Innovation Research ISI. Optimized pathways towards ambitious climate protection in the european electricity system (eu long-term scenarios 2050 ii). Technical report; 2014.
[44] NREL. NREL 2018 Annual Technology Baseline; 2018. https://atb.nrel.gov/.
[45] Buttler A, Spliethoff H. Current status of water electrolysis for energy storage, grid balancing and sector coupling via power-to-gas and power-to-liquids: A review. Renew Sustain Energy Rev 2018;82:2440–54.
[46] Fuel Cells and Hydrogen Joint Undertaking (FCH JU). Addendum to the multi-annual work plan 2014-2020; 2018. https://www.fch.europa.eu/sites/default/files/MAWP%20final%20version_endorsed%20GB%2015062018%20%28ID%203712421%29.pdf.
[47] International Energy Agency (IEA), The future of hydrogen, June 2019. https://www.iea.org/reports/the-future-of-hydrogen.
[48] Schmidt O, Gambhir A, Staffell I, Hawkes A, Nelson J, Few S. Future cost and performance of water electrolysis: an expert elicitation study. Int. J. Hydrogen Energy 2017;42(52):30470–92.
[49] Pratt J, Terlip D, Ainscough C, Kurtz J, Elgowainy A. H2first reference station design task: Project deliverable 2–2. Technical report, National Renewable Energy Lab. (NREL), Golden, CO (United States); 2015.
[50] Fuel Cell Technologies Office (FCTO). Multi-year research development, and demonstration plan, section 3.2 hydrogen delivery. Technical report, U.S. Department of Energy (DOE); 2015.
[51] Wilson A, Kleen G, Papageorgopoulos D. Fuel cell system cost – 2017. DOE Hydrogen and Fuel Cells Program Record # 17007; 2017.
[52] Trade Ministry of Economy and Industry Japan. New era of a hydrogen energy society; 2018. http://injapan.no/wp-content/uploads/2018/03/180227_METI-New-Era-of-a-Hydrogen-Energy-Society.pdf.
[53] Staffell I, Green R. The cost of domestic fuel cell micro-chp systems. Int J Hydrogen Energy 2013;38:1088–102.
[54] Sandvall AF, Ahlgren EO, Ekvall T. Cost-efficiency of urban heating strategies modelling scale effects of low-energy building heat supply. Energy Strategy Rev 2017;18:212–23.
[55] US Energy Information Administration (EIA). Updated buildings sector appliance and equipment costs and efficiencies; 2018. https://www.eia.gov/analysis/studies/buildings/equipcosts/pdf/full.pdf.
[56] Schüppler S, Fleuchaus P, Blum P. Techno-economic and environmental analysis of an aquifer thermal energy storage (ates) in germany. Geothermal Energy 2019;7(1):11.
[57] Bloomberg Finance. New energy outlook 2018; 2018. https://bnef.turtl.co/story/neo2018?src=Website&teaser=true.
[58] Bunsen T, Cazzola P, Gorner M, Paoli L, Scheffer S, Schuitmaker R, Tattini J, Teter J. Global EV Outlook 2018: Towards cross-modal electrification. International Energy Agency; 2018.
[59] Berckmans G, Messagie M, Smekens J, Omar N, Vanhaverbeke L, Van Mierlo J. Cost projection of state of the art lithium-ion batteries for electric vehicles up to 2030. Energies 2017;10(9):1314.
[60] Hinkley J, Hayward J, McNaughton R, Gillespie R, Matsumoto A, Watt M, Lovegrove K. Cost assessment of hydrogen production from pv and electrolysis. CSIRO Australia; 2016.
[61] Pawel I. The cost of storage–how to calculate the levelized cost of stored energy (lcoe) and applications to renewable energy generation. Energy Procedia 2014;46:68–77.
[62] Hesse H, Schimpe M, Kucevic D, Jossen A. Lithium-ion battery storage for the grida review of stationary battery storage system design tailored for applications in modern power grids. Energies 2017;10:2107.
[63] Körner A, Tam C, Bennett S, Gagné JF. Technology roadmap-hydrogen and fuel cells. International Energy Agency (IEA): Paris, France; 2015.
[64] Everoze and EVConsult. V2G global roadtrip: Around the world in 50 projects. an everoze & evconsult report jointly commissioned by uk power networksand innovate uklessons learned from fifty international vehicle-to-grid projects; 2018. https://www.evconsult.nl/wp-content/uploads/2018/10/Final-Report-UKPN001-S-01-I-V2G-global-review.pdf.
[65] Robinius M, Linssen J, Grube T, Reu M, Stenzel P, Syranidis K, Kuckertz P, Stolten D. Comparative analysis of infrastructures: hydrogen fueling and electric charging of vehicles. Forschungszentrum Jlich GmbH Zentralbibliothek 2018.